

1 **The effect of emission source chemical profiles on simulated PM<sub>2.5</sub> components:**  
2 **sensitivity analysis with CMAQv5.0.2**

3 Zhongwei Luo<sup>a,b,1</sup>, Yan Han<sup>a,b,c,1</sup>, Kun Hua<sup>a,b</sup>, Yufen Zhang<sup>a,b\*</sup>, Jianhui Wu<sup>a,b</sup>, Xiaohui  
4 Bi<sup>a,b</sup>, Qili Dai<sup>a,b</sup>, Baoshuang Liu<sup>a,b</sup>, Yang Chen<sup>c</sup>, Xin Long<sup>c</sup>, Yinchang Feng<sup>a,b\*</sup>

5 <sup>a</sup>State Environmental Protection Key Laboratory of Urban Ambient Air Particulate  
6 Matter Pollution Prevention and Control & Tianjin Key Laboratory of Urban  
7 Transport Emission Research, College of Environmental Science and Engineering,  
8 Nankai University, Tianjin 300350, China.

9 <sup>b</sup>CMA-NKU Cooperative Laboratory for Atmospheric Environment-Health Research,  
10 Tianjin 300350, China.

11 <sup>c</sup>Research Center for Atmospheric Environment, Chongqing Institute of Green and  
12 Intelligent Technology, Chinese Academy of Sciences, Chongqing 400714, China.

13

14

15 \*Corresponding authors:

16 Y. F. Zhang (zhafox@nankai.edu.cn). And Y. C. Feng (fengyc@nankai.edu.cn).

17

18 <sup>1</sup>Z. W. Luo and Y. Han equally contribute to this work

19 **Abstract**

20 The chemical transport model (CTM) is an essential tool for air quality prediction  
21 and management, widely used in air pollution control and health risk assessment.  
22 However, the current models do not perform very well in reproducing the observations  
23 of some major chemical components, for example, sulfate, nitrate, ammonium and  
24 organic carbon. Studies suggested that the uncertainties of model chemical mechanism,  
25 source emission inventory and meteorological field can cause inaccurate simulation  
26 results. Still, the emission source profile (used to create speciated emission inventories  
27 for CTMs) of PM<sub>2.5</sub> has not been fully taken into account in current numerical  
28 simulation. Based on the characteristics and variation rules of chemical components in  
29 typical PM<sub>2.5</sub> sources, different simulation scenarios were designed and the sensitivity  
30 of simulated PM<sub>2.5</sub> components to source chemical profile was explored. Our findings  
31 showed that the influence of source profile changes on simulated PM<sub>2.5</sub> components'  
32 concentrations could not be ignored. Simulation results of some components were  
33 sensitive to the adopted source profile in CTMs. Moreover, there was a linkage effect,  
34 the variation of some components in the source profile would bring changes to the  
35 simulated results of other components. These influences are connected to chemical  
36 mechanisms of the model since the variation of species allocations in emission sources  
37 can affect potential composition and phase state of aerosols, chemical reaction priority  
38 and multicomponent chemical balance in thermodynamic equilibrium system. We also  
39 found that the perturbation of PM<sub>2.5</sub> source profile caused the variation of simulated  
40 gaseous pollutants, which indirectly indicated that the perturbation of source profile  
41 would affect the simulation of secondary PM<sub>2.5</sub> components. Our paper highlights the  
42 necessity that the representativeness and timeliness of the source profile should be paid  
43 enough attention when using CTMs for simulation.

44 **Keywords**

45 PM<sub>2.5</sub>; source profile; component; numerical simulation; chemical transport model

## 46 **1. Introduction**

47 Ambient fine particulate matter (PM<sub>2.5</sub>) pollution in some key regions of China  
48 has attracted much attention (Liang et al., 2020; Huang et al., 2021). The chemical  
49 components of PM<sub>2.5</sub>, including elements (Al, Si, Fe, Mn, Ti, Cu, Zn, Pb, etc.), water-  
50 soluble ions (SO<sub>4</sub><sup>2-</sup>, NO<sub>3</sub><sup>-</sup>, Cl<sup>-</sup>, F<sup>-</sup>, NH<sub>4</sub><sup>+</sup>, Na<sup>+</sup>, K<sup>+</sup>, Mg<sup>2+</sup>, Ca<sup>2+</sup>, etc.), and carbon-  
51 containing components (Organic Carbon, OC; Elemental Carbon, EC) (Yang et al.,  
52 2011; Li et al., 2013), have different physical and chemical properties, such as reactivity,  
53 thermal stability, particle size distribution, residence time, optical properties, health  
54 hazards, etc (Seinfeld and Pandis, 2006; Tang et al., 2006). According to long-term  
55 monitoring results, in most regions of China, SO<sub>4</sub><sup>2-</sup>, NO<sub>3</sub><sup>-</sup>, NH<sub>4</sub><sup>+</sup> and OC are the most  
56 important species in ambient PM<sub>2.5</sub> (Li et al., 2017a; Li et al., 2021), which has a certain  
57 adverse impact on human health (Shi et al., 2018) and ecosystem, such as acid rain in  
58 southwest China (Han et al., 2019), food security (Zhou et al., 2018), etc.

59 The chemical transport models (CTMs) play an important role in policy making  
60 for regulatory purposes. Based on the scientific understanding of atmospheric physical  
61 and chemical processes, CTMs are built to simulate the transport, reaction and removal  
62 of pollutants on a certain scale in horizontal and vertical directions. With the  
63 development of CTMs, the simulation accuracy of PM<sub>2.5</sub> concentration has been  
64 significantly improved. Higher requirements have been put forward for the precise  
65 simulation of PM<sub>2.5</sub> components so as to provide support for the use of CTMs in human  
66 health risk assessment, climate effects, pollution sources apportionment, and so on  
67 (Peterson et al., 2020; Lv et al., 2021). However, the current models perform not very  
68 well in simulating some components (for example, PM<sub>2.5</sub>-bound sulfate, nitrate,  
69 ammonium, trace elements, etc.) (Zheng et al., 2015; Fu et al., 2016; Ying et al., 2018;  
70 Cao et al., 2021). In the current literatures, the correlation coefficient (R) and  
71 normalized mean bias (NMB) are highly variable and inconsistent between the  
72 simulated and the observed values (listed in Table S1). This is mainly attributable to the  
73 uncertainties of model chemical mechanism, source emission inventory and

74 meteorological field simulation.

75 The chemical mechanisms involved in CTMs are derived from parameterized  
76 assumptions based on laboratory simulation and field observations. The actual  
77 atmospheric chemical processes are very complex, and some reaction mechanisms are  
78 still limitedly understood. In addition, the integration of chemical reactions and  
79 simplified treatment methods in the model cannot fully reflect the correlation among  
80 atmospheric pollutants. For example, in some model mechanisms, important sulfate and  
81 nitrate formation pathways through new heterogeneous chemistry were added,  
82 including the chemical reaction between SO<sub>2</sub> and aerosol, NO<sub>2</sub>/NO<sub>3</sub>/N<sub>2</sub>O<sub>3</sub> and aerosol  
83 (Zheng et al., 2015), nitrous acid oxidized SO<sub>2</sub> to produce sulfate (Zheng et al., 2020),  
84 dust particles promoted the oxidation of SO<sub>2</sub> (Yu et al., 2020), modified the uptake  
85 coefficients for heterogeneous oxidation of SO<sub>2</sub> to sulfate (Zhang et al., 2019), updated  
86 the heterogeneous N<sub>2</sub>O<sub>5</sub> parameterization (Foley et al., 2010). Even though the  
87 aforementioned processes can significantly improve the simulation of SO<sub>4</sub><sup>2-</sup> and NO<sub>3</sub><sup>-</sup>,  
88 there is still a gap between the modeled and the actual atmospheric chemical processes.

89 The uncertainty of meteorological field simulation is another crucial reason for the  
90 simulation deviation, especially on heavy pollution days, the variation trends of PM<sub>2.5</sub>  
91 chemical components were not well-captured (Ying et al., 2018; Qi et al., 2019; Wang  
92 et al., 2022). Precipitation is the key meteorological factor determining wet removal of  
93 pollutants; boundary layer height and wind speed are the main factors affecting  
94 convection and transport of pollutants; solar radiation, temperature and relative  
95 humidity are the key factors affecting the formation of secondary particles (Huang et  
96 al., 2019; Chen et al., 2020). Some literature reported that deviation from precipitation  
97 and wind field simulation might lead to underestimation of SO<sub>4</sub><sup>2-</sup>, NO<sub>3</sub><sup>-</sup> and NH<sub>4</sub><sup>+</sup>  
98 (Cheng et al., 2015; Zhang et al., 2017). Devaluation of liquid water path and cloud  
99 cover cause a decrease of sulfate formation in cloud, and ultimately results in  
100 significantly underestimated components in simulation values (Sha et al., 2019; Foley  
101 et al., 2010). Underestimation of temperature and relative humidity may also cause  
102 adverse effects of temperature- and/or relative humidity-dependence chemical reaction

103 in the simulation (Sha et al., 2019).

104 The uncertainty of source emission inventory also significantly affects the  
105 simulation results of PM<sub>2.5</sub> components (Shi et al., 2017; Sha et al., 2019). Due to  
106 incomplete information or insufficient representativeness, pollutant emissions are  
107 sometimes overestimated or underestimated, and the method for temporal and spatial  
108 allocation also needs to be improved.

109 In particular, the emission source profile of PM<sub>2.5</sub> (Hereinafter referred to as  
110 "source profile"), used to create speciated emission inventories for CTMs (Hsu et al.,  
111 2019), has not been fully taken into account in the current numerical simulation. In the  
112 reported literatures, PM<sub>2.5</sub> species allocation coefficients of emission sources are  
113 commonly treated in the following ways: (1) allocated PM<sub>2.5</sub> components of source  
114 emissions by referring to source profile data in published literature or database like the  
115 US SPECIATE (Fu et al., 2013; Wang et al., 2014; Ying et al., 2018); (2) chemical  
116 profiles come from local measurement (Fu et al., 2013; Appel et al., 2013). However,  
117 with the development of production technology and the innovation of pollution  
118 treatment technology in recent years, some source profiles have changed dramatically  
119 (Bi et al., 2019), such as SO<sub>4</sub><sup>2-</sup> from coal burning, its content in PM<sub>2.5</sub> is generally low  
120 in coal-fired power plant without desulfurizing facilities, while existing coal-fired  
121 power plants using limestone/gypsum wet desulphurization, the contents of SO<sub>4</sub><sup>2-</sup> in  
122 PM<sub>2.5</sub> are significantly higher than that without desulfurization facilities (Zhang et al.,  
123 2020). The timeliness of PM<sub>2.5</sub> species allocation coefficients in current CTMs also  
124 needs to be considered.

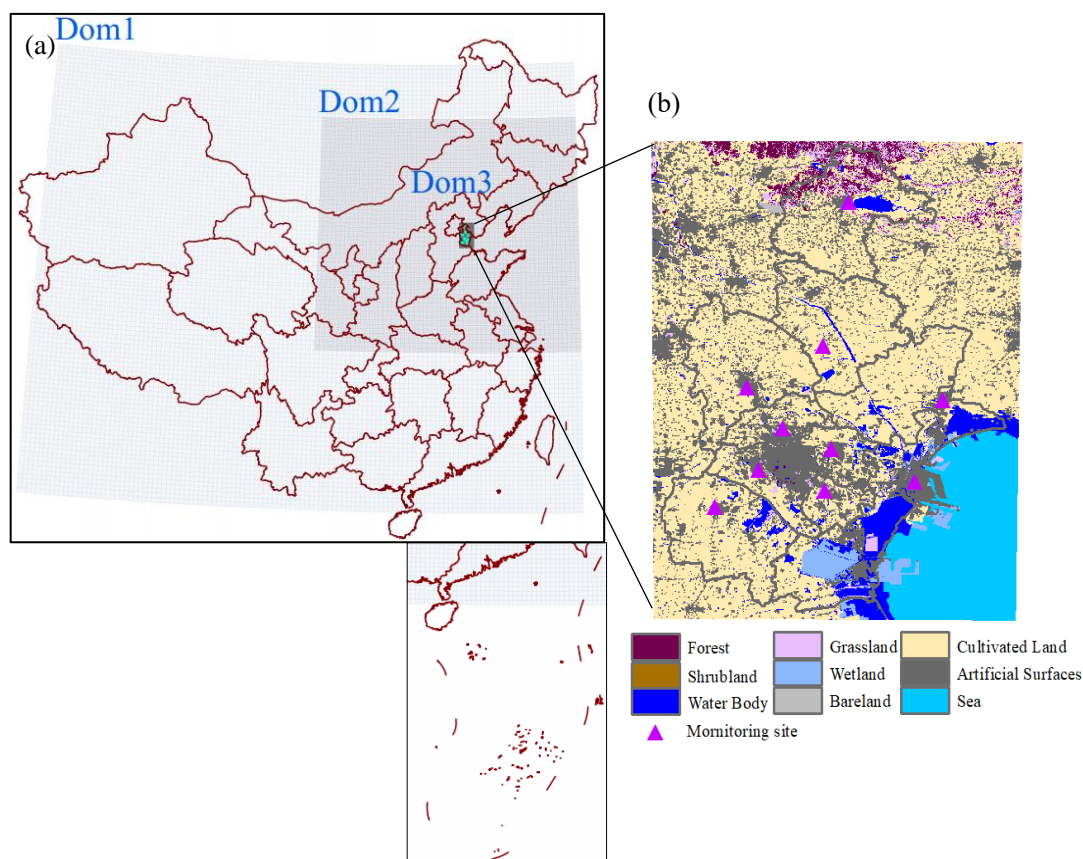
125 This paper attempts to answer the following questions: (1) Whether the variation  
126 of the source profile adopted in the model has an impact on the simulated results of  
127 PM<sub>2.5</sub> chemical components? (2) How much does it impact? (3) How does the impact  
128 work? Aiming at these problems above, chemical composition and its variation law for  
129 typical PM<sub>2.5</sub> emission sources are summarized, on this basis, sensitivity tests are  
130 designed to identify whether PM<sub>2.5</sub> source profiles and species allocation in the model  
131 are important parameters that affect the simulation results of chemical components'

132 concentrations in PM<sub>2.5</sub>. We take CMAQ (one of the most widely used CTMs), MEIC  
133 (a high-resolution inventory of anthropogenic air pollutants in China) as the carriers.  
134 The same kind of experiment is also applicable to other CTMs and emission inventories.  
135 The aim of this study is to provide support for the effective utilization of source profiles  
136 in the CTMs and improvement of the simulation schemes.

## 137 **2. Model and Data**

### 138 **2.1 Model configuration**

139 Weather Research and Forecasting model (WRF-3.7.1), the widely used  
140 Community Multiscale Air Quality model (CMAQv5.0.2) (Eder and Yu, 2006; Yu et al.,  
141 2014), and Multi-resolution Emission Inventory for China (MEICv1.3) have been used  
142 in this study. MEIC, developed by Tsinghua University, mainly tracked anthropogenic  
143 emissions in China including coal-fired power plants, industry, vehicles, residents and  
144 agriculture ([http://meicmodel.org/?page\\_id=135](http://meicmodel.org/?page_id=135)) (Li et al., 2017b; Zheng et al., 2018).  
145 The WRF model was used to generate meteorological inputs for the CMAQ model.  
146 Three nested modeling domains consisting of 36 km×36 km (Dom1), 12 km×12km  
147 (Dom2), and 4 km×4km (Dom3) horizontal grid sizes were set, as shown in Fig. 1. The  
148 initial and boundary conditions for WRF were based on the North American Regional  
149 Reanalysis data archived at National Center for Atmospheric Research (NCAR). In  
150 addition, surface and upper air observations obtained from NCAR were used to further  
151 refine the analysis data. The modeling was conducted from Oct. 1 to Oct.30 in 2018,  
152 and major configurations we used in CMAQ were illuminated as follows: Gas-phase  
153 chemistry was based on the CB05 mechanism and the aerosol dynamics/chemistry was  
154 based on the aero6 module (cb05tucl\_ae6\_aq). The detailed model configurations were  
155 shown in Table S2, and regional distribution of PM<sub>2.5</sub> emission sources were shown in  
156 Figure S1.



157  
 158 Fig.1 Modeling domains of the CMAQ model. (a) The three-domain nested CMAQ domains; (b)  
 159 Land use and observation sites of Dom3 (Data source of Land use: GLOBELAND30,  
 160 www.globeland30.org, National Geomatics Center of China).

## 161 2.2 Selection and comparison of PM<sub>2.5</sub> emission source profile

162 The PM<sub>2.5</sub> emission source profiles from database of Source Profiles of Air  
 163 Pollution (SPAP) (<http://www.nkspap.com:9091/>), U.S. Environmental Protection  
 164 Agency's (EPA) SPECIATE database ([https://www.epa.gov/air-emissions-  
 165 modeling/speciate](https://www.epa.gov/air-emissions-modeling/speciate)) as well as from published literature were selected, respectively. The  
 166 SPAP was developed by the State Environment Protection Key Laboratory of Urban  
 167 Particulate Air Pollution Prevention, Nankai University, China. This database contains  
 168 more than 3000 size-resolved source profiles of stationary combustion sources,  
 169 industrial processes, vehicle exhaust, biomass burning, dust and other sources, collected  
 170 from more than 40 cities in China since 2001. In addition to inorganic elements, water-  
 171 soluble ions, OC, EC and other conventional components, some source profiles also  
 172 encompass a series of tracer information, such as organic markers, isotopes, single  
 173 particle mass spectrometry, VOCs and other gaseous precursors. Based on species in

174 the aerosol chemical mechanism (AERO6) of CMAQ (Appel et al., 2013; Chapel Hill,  
 175 2012), we selected 15 components in PM<sub>2.5</sub> source profiles including Al, Ca, Cl, EC,  
 176 Fe, K, Mg, Mn, Na, OC, Si, Ti, NH<sub>4</sub><sup>+</sup>, NO<sub>3</sub><sup>-</sup> and SO<sub>4</sub><sup>2-</sup>, the remaining components are  
 177 classified as “other”. In the database of Source Profiles of Air Pollution (SPAP) and  
 178 U.S. Environmental Protection Agency’s (EPA) SPECIATE database, these four source  
 179 categories (coal-fired power plant, industry process, transportation sector and  
 180 residential coal combustion) contain a series of sub-categories. But the MEIC emission  
 181 inventory does not include the corresponding sub-categories. So we take the average  
 182 values of source profiles in each source category as representing source profile, the  
 183 details could also be seen in our previous work (Bi et al., 2019); Then multiply  
 184 inventory emissions by profile fraction to get emissions of specific chemical  
 185 components.

186 To determine the similarity between the two groups of source profiles, Coefficient  
 187 Divergence (CD) is calculated using the following formula (Wongphatarakul et al.,  
 188 1998):

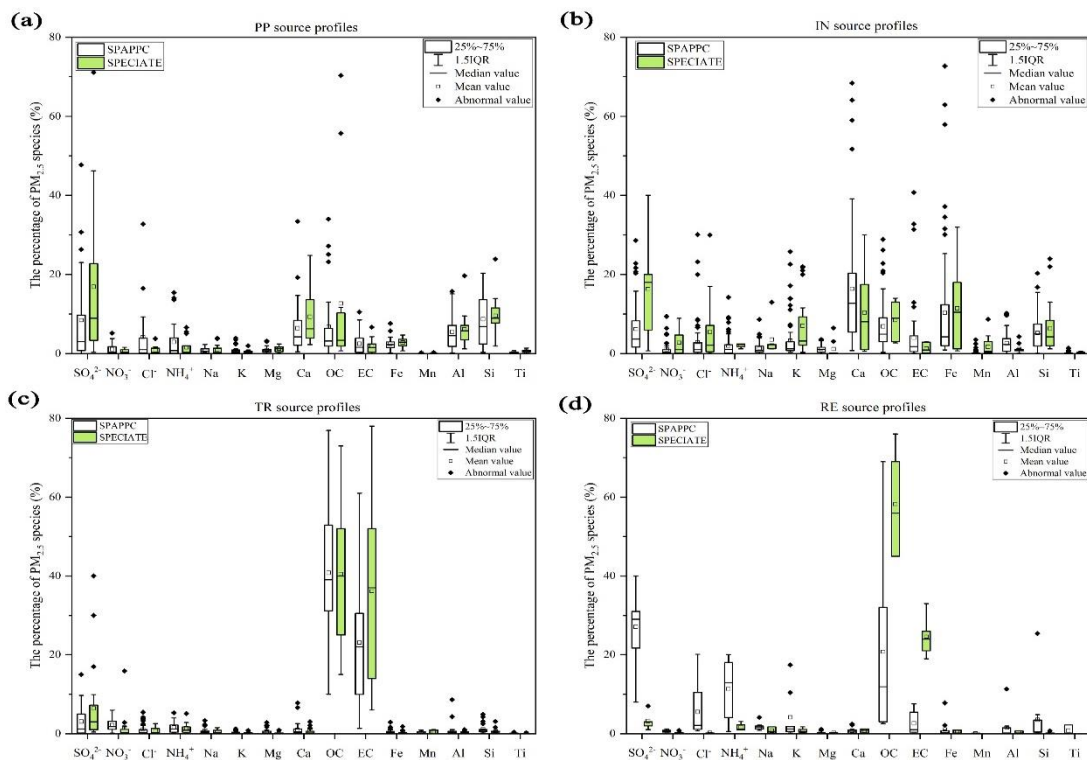
$$189 \quad CD_{jk} = \sqrt{\frac{1}{p} \sum_{i=1}^p \left( \frac{x_{ij} - x_{ik}}{x_{ij} + x_{ik}} \right)^2} \dots\dots\dots (1)$$

190 Where CD<sub>jk</sub> is the coefficient of divergence of source profile *j* and *k*, *p* is the  
 191 number of chemical components in source profile, *x<sub>ij</sub>* is the weight percentage for  
 192 chemical component *i* in source profile *j*, *x<sub>ik</sub>* is the weight percentage for *i* in source  
 193 profile *k* (%). The CD value is in the range of 0 to 1, if the two source profiles are  
 194 similar, the value of CD is close to 0; if the two are very different, the value is close to  
 195 1.

196 **Coal-fired power plant (PP).** Coal-fired power plants remain the main coal  
 197 consumers in China, which accounted for 50.2% of total coal consumption in 2019  
 198 (NBS, 2021) and gained much more attention, especially with the wide implementation  
 199 of the ultralow emission standards, PM<sub>2.5</sub> emission characteristics have changed  
 200 accordingly (Wu et al., 2020; Wu et al., 2022). There are obvious differences in PM<sub>2.5</sub>  
 201 source profiles between SPAPPC (SPAP database and published source profiles in



202 China) and SPECIATE (U.S.EPA SPECIATE database), the CD value of these two  
 203 groups lie between 0.34 and 0.92 ( $0.64\pm 0.10$ ), detailed information is shown in Table  
 204 S3 and Figure S2. The percentages of species in PP source profiles are plotted in Fig.  
 205 2(a). The main components in SPAPPC are sorted by Si,  $\text{SO}_4^{2-}$ , OC, Ca with average  
 206 values of  $8.7\pm 6.8\%$ ,  $8.5\pm 11.5\%$ ,  $6.8\pm 9.1\%$  and  $6.5\pm 6.9\%$ , respectively; The SPECIATE  
 207 are enriched in  $\text{SO}_4^{2-}$  ( $16.9\%\pm 20.0\%$ ), OC ( $12.7\%\pm 21.8\%$ ), Si ( $9.6\pm 5.0\%$ ) and Ca  
 208 ( $9.3\pm 7.3\%$ ), higher than SPAPPC. Coal properties, burning conditions, pollution control  
 209 measures and emission sampling methods are the main reasons for those great  
 210 percentage fluctuations. Different treatment processes of flue gases, e.g. wet/dry  
 211 limestone, ammonia and double-alkali flue gas desulfurization, will affect the  
 212 percentages of components in source profiles (Zhang et al., 2020). It has been reported  
 213 that the percentage of Ca, Mg,  $\text{SO}_4^{2-}$  and  $\text{Cl}^-$  in PP profiles increased after the limestone-  
 214 gypsum method was used in coal-fired power plants (Bi et al., 2019). Besides that, the  
 215 percentage of  $\text{Cl}^-$  in SPAPPC is obviously higher than that in SPECIATE, which might  
 216 attribute to the generally higher  $\text{Cl}^-$  content in raw coal in China (Guo et al., 2004).



217  
 218 Fig. 2 Chemical profiles for  $\text{PM}_{2.5}$  emitted from (a) coal-fired power plants (PP), (b) industry  
 219 processes (IN), (c) transportation sector (TR), (d) residential coal combustion (RE). Data obtained

220 from SPAPPC (SPAP database and published source profiles in China) and SPECIATE (U.S. EPA  
221 SPECIATE database)

222 **Industrial process(IN).** Industrial emissions are one of the major sources of PM<sub>2.5</sub>  
223 (Hopke et al., 2020), the percentages of Ca, Fe, OC and SO<sub>4</sub><sup>2-</sup> are relatively high both  
224 in SPAPPC and SPECIATE, but the shares in different source profile database varied,  
225 their CD values vary from 0.45 to 0.94 (0.72±0.09) (Detailed information were shown  
226 in Table S4~S7 and Figure S3). In SPAPPC, these four components account for  
227 16.4±14.9%, 10.4±14.4%, 6.9±6.1%, 6.2±6.4%, the proportions in SPECIATE are  
228 10.4±9.8%, 11.4±10.6%, 8.5±4.9%, 16.3±13.3%, respectively (Fig. 2(b)). Large  
229 variations of components and their percentages in industrial processes are attributed to  
230 the manufacturing processes, raw material, pollution control measures and so on (Ji et  
231 al., 2017; Bi et al., 2019; Gao et al., 2022). For example, Ca, Al, OC and SO<sub>4</sub><sup>2-</sup> are found  
232 to have the highest percentage in cement sources (Guo et al., 2021); Fe, Si and SO<sub>4</sub><sup>2-</sup>  
233 are the most abundant species in steel industry emission (Guo et al., 2017).

234 **Transportation sector (TR).** Traffic contributed a large fraction of PM<sub>2.5</sub> in many  
235 locations (Hopke et al., 2022). It is well-known that the transportation sector makes a  
236 dominant contribution of OC and EC. The main components of PM<sub>2.5</sub> emitted from  
237 traffic sources are OC, EC and SO<sub>4</sub><sup>2-</sup> both in SPAPPC and SPECIATE, but still vary in  
238 wide range, their CD values fall between 0.33 and 0.86 (0.69±0.09) (Detailed  
239 information was given in Table S8~S10 and Figure S4). In SPAPPC, the percentages of  
240 OC, EC and SO<sub>4</sub><sup>2-</sup> are 40.8±15.0%, 23.1±13.8%, 3.1±3.7%, and in SPECIATE, the  
241 percentages are 40.6±16.4%, 36.1±21.5%, 6.4±9.9%, respectively (Fig. 2(c)). These  
242 significant differences mainly attribute to the vehicle type, fuel quality, mixing ratio  
243 between oil and gas and the combustion phase in vehicle engine and so on (Xia et al.,  
244 2017).

245 **Residential coal combustion (RE).** Residential coal combustion, as the leading  
246 source of global PM<sub>2.5</sub> emission (Weagle et al., 2018), has a much higher emission  
247 factor than coal-fired power plant (Wu et al., 2022). The fraction of components vary  
248 greatly in the profiles measured from SPAPPC and SPECIATE, their CD values are  
249 0.75±0.10 (Detailed information was given in Table S11 and Figure S5), SO<sub>4</sub><sup>2-</sup>, OC,

250  $\text{NH}_4^+$  and EC make the main contribution to  $\text{PM}_{2.5}$  emitted from residential coal  
251 combustion. In SPAPPC, the average percentages of  $\text{SO}_4^{2-}$ , OC,  $\text{NH}_4^+$ , EC are  
252  $27.1\pm 10.1\%$ ,  $20.7\pm 20.6\%$ ,  $11.3\pm 7.7\%$ ,  $2.6\pm 2.8\%$ , respectively. In SPECIATE, the  
253 average percentages are OC ( $58.2\pm 14.0\%$ ), EC ( $24.6\pm 5.4\%$ ),  $\text{SO}_4^{2-}$  ( $3.2\pm 2.3\%$ ) and  
254  $\text{NH}_4^+$  ( $1.6\pm 1.0\%$ ) (Fig. 2(d)). Total percentages of OC and EC in SPECIATE are over  
255 80%, obviously higher than that in SPAPPC, while a higher percentage of  $\text{SO}_4^{2-}$ , Cl<sup>-</sup>, K  
256 and Si are observed in SPAPPC. The coal type and properties, burning condition are the  
257 main factors affecting the percentages of  $\text{PM}_{2.5}$  components, like the chunk coal burning  
258 has relatively higher percentages of OC, EC,  $\text{SO}_4^{2-}$ ,  $\text{NO}_3^-$  and  $\text{NH}_4^+$  than honeycomb  
259 briquette (Wu et al., 2021; Song et al., 2021).

260 Briefly, many factors can affect  $\text{PM}_{2.5}$  source profiles, and with the innovation of  
261 manufacturing technique and pollution control technology, changes in fuel and raw and  
262 auxiliary materials, the main chemical components and their percentages would change  
263 dramatically. To explore whether the variations of source profile adopted in CMAQ  
264 model would be one of the important factors affecting the simulated  $\text{PM}_{2.5}$  component,  
265 we designed a series of simulation tests to address the following issues.

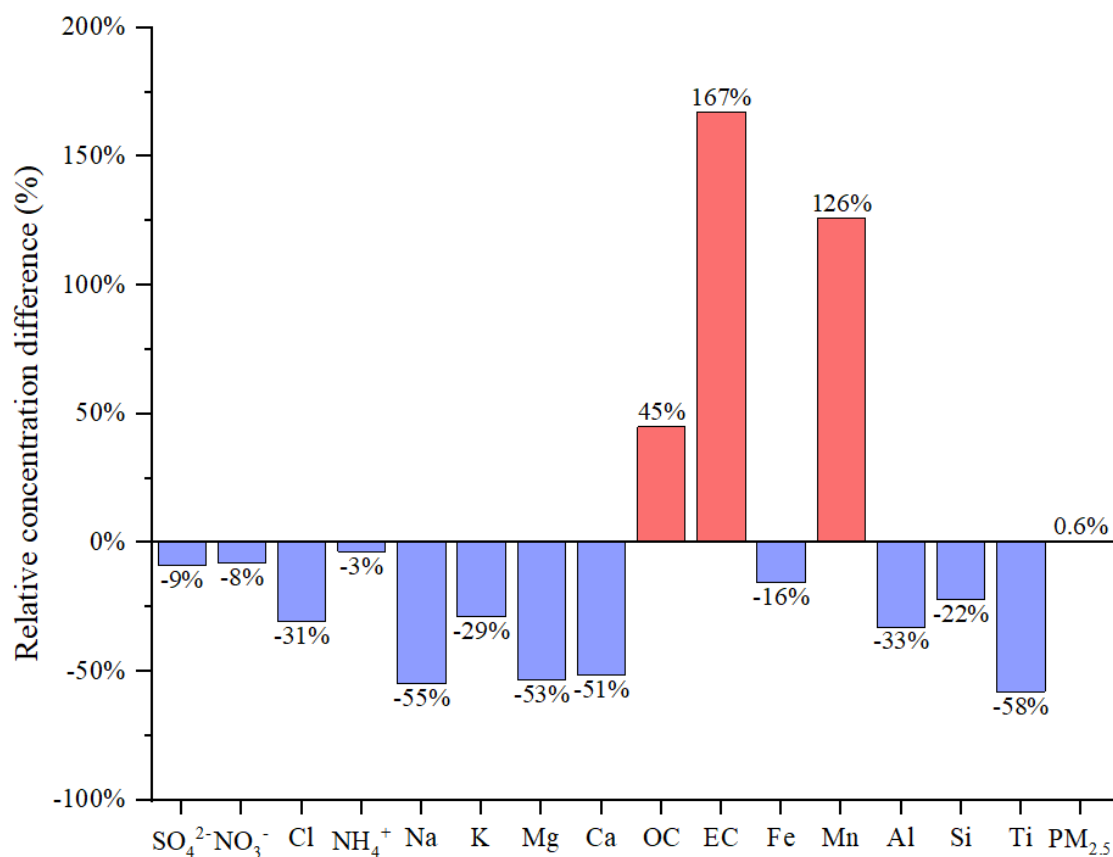
### 266 **3 Is there an impact of variation of source profile on the simulation results?**

267 In this part, we separately selected source profiles from SPAPPC and SPECIATE  
268 databases and applied them in emission inventory for simulating  $\text{PM}_{2.5}$  and its  
269 components with other modeling conditions unchanged, corresponding to case  
270 CMAQ\_SPA and CMAQ\_SPE. The detail information of source profiles were shown  
271 in Figure S6.

272 By comparing the selected SPAPPC source profiles with the selected SPECIATE  
273 source profiles, the coefficient divergences for the four main source categories were  
274  $\text{CD}_{\text{PP}}(0.67) > \text{CD}_{\text{RE}}(0.62) > \text{CD}_{\text{TR}}(0.60) > \text{CD}_{\text{IN}}(0.60)$ , which meant the selected source  
275 profiles in the two simulation cases were quite different. The average simulated  
276 concentration of  $\text{PM}_{2.5}$  and its components at each ambient air quality monitoring  
277 station (Table S12) were extracted from CMAQ outputs. We selected one air quality

278 monitoring station (Site 8 as the selected station here and any site could be available)  
 279 to explore the effect of emission source chemical profiles on simulated PM<sub>2.5</sub>  
 280 components, then used the left 9 sites to further illustrate the conclusions suggested.

281 The simulation results for PM<sub>2.5</sub> species under CMAQ\_SPA and CMAQ\_SPE  
 282 cases also showed big differences (as shown in Fig. 3 and Table S13). The largest  
 283 difference in average simulated concentration was EC with CAMQ\_SPE giving higher  
 284 by 167% than CMAQ\_SPA; For OC and Mn, higher values were also given by  
 285 CMAQ\_SPE than by CMAQ\_SPA (45% and 126% on average, respectively); For the  
 286 other components of concern, the simulated concentration by CMAQ\_SPE was lower  
 287 than CMAQ\_SPA with Ti (58%), Na (55%), Mg (53%), Ca (51%), Al (33%), Cl (31%),  
 288 K (29%), Si (22%), Fe (16%), NH<sub>4</sub><sup>+</sup> (3%), SO<sub>4</sub><sup>2-</sup> (9%), NO<sub>3</sub><sup>-</sup> (8%), separately. While the  
 289 simulated PM<sub>2.5</sub> concentrations under the two cases were quite close. The influence of  
 290 source profile variation on the simulated PM<sub>2.5</sub> concentration was not significant, but  
 291 the influence on the simulation of chemical components in PM<sub>2.5</sub> could not be ignored.



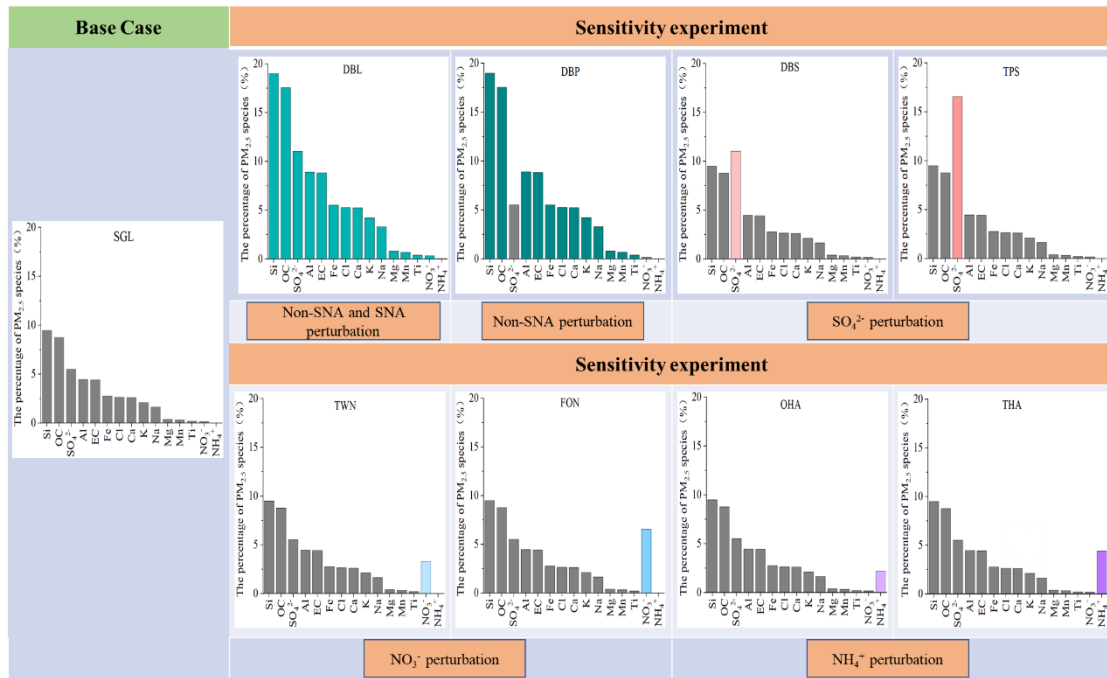
292

293 Fig. 3 The relative concentration difference of average simulated results (PM<sub>2.5</sub> and its components)

294 between CMAQ\_SPE and CAMQ\_SPA (relative to CAMQ\_SPA) during simulation period; PM<sub>2.5</sub>  
 295 source profiles from SPAPPC and SPECIATE database were used to create speciated emission  
 296 inventories for CMAQ, corresponding to case CMAQ\_SPA and CMAQ\_SPE, respectively.

297 **4 How much does it impact?**

298 To quantitatively characterize how much the source profiles affect the simulation  
 299 results, we selected the chemical composition of code 000002.5 (Variety of different  
 300 categories, used for the overall average composite profiles (Hsu et al., 2019) in the US  
 301 EPA Speciate\_5.0\_0 database for species allocation of PM<sub>2.5</sub> components. The  
 302 corresponding percentages of EC, OC, Mn, Fe, Ti, Al, Si, Ca, Mg, K, Na, Cl, NH<sub>4</sub><sup>+</sup>,  
 303 NO<sub>3</sub><sup>-</sup> and SO<sub>4</sub><sup>2-</sup> in PM<sub>2.5</sub> were shown in Fig. 4 (SGL, base case simulation).



304  
 305 Fig. 4 The general roadmap of sensitivity tests (The histogram in each case were the speciation  
 306 profile in CTMs; SNA represented SO<sub>4</sub><sup>2-</sup>, NO<sub>3</sub><sup>-</sup>, and NH<sub>4</sub><sup>+</sup>, Non-SNA represented other components  
 307 in PM<sub>2.5</sub>).

308 Table 1 The content of sensitivity experiment cases

| Experiment Cases   | Description <sup>3</sup>   |
|--|--|
| Case DBL:<br>add perturbation to Non-SNA<br>and SNA <sup>1</sup> | The percentage of all the listed components in the source profile of base case (SGL) were doubled, and the proportion of unlisted components (Other) <sup>2</sup> decreased to 9%. |
| Case DBP:  | The percentages of non-SNA were doubled and SNA( SO <sub>4</sub> <sup>2-</sup> ,   |

|  |  |
|--|--|
| add perturbation to Non-SNA  | NO <sub>3</sub> <sup>-</sup> , NH <sub>4</sub> <sup>+</sup> ) species stayed the same with that in SGL (the cumulative percentage of listed species was 85.3%), the proportion of unlisted components decreased to 14.7%.  |
| Case DBS and TPS:<br>add perturbation to SO <sub>4</sub> <sup>2-</sup> | The percentage of SO <sub>4</sub> <sup>2-</sup> was doubled (11%, DBS, represented Double Sulfate), tripled (16.5%, TPS, represented Triple Sulfate) and the other listed 14 species stayed the same with that in SGL (the cumulative percentage of listed species was 51% and 57%, respectively), the proportion of unlisted components decreased to 49% and 43%. |
| Case TWN and FON:<br>add perturbation to NO <sub>3</sub> <sup>-</sup>  | The NO <sub>3</sub> <sup>-</sup> content was raised up to 20 times (3.3%, TWN) and 40 times (6.6%, FON) of that in SGL (0.16%), the other 14 species stayed the same with SGL (the cumulative percentage of listed species was 48.6% and 51.9%, respectively), the proportion of unlisted components decreased to 51.4% and 48.1%.                                 |
| Case OHA and THA:<br>add perturbation to NH <sub>4</sub> <sup>+</sup>  | The NH <sub>4</sub> <sup>+</sup> content was raised up to 100 times (2.2%, OHA), 200 times (4.4%, THA) of that in SGL (0.02%), the other 14 species stayed the same with SGL (the cumulative percentage of listed species was 47.7% and 49.9%, respectively), the proportion of unlisted components decreased to 52.3% and 50.1%.                                  |

Note:

1. SNA represented SO<sub>4</sub><sup>2-</sup>, NO<sub>3</sub><sup>-</sup>, and NH<sub>4</sub><sup>+</sup>, Non-SNA represented other components in PM<sub>2.5</sub>.
2. The listed components contained Al, Ca, Cl, EC, Fe, K, Mg, Mn, Na, OC, Si, Ti, NH<sub>4</sub><sup>+</sup>, NO<sub>3</sub><sup>-</sup> and SO<sub>4</sub><sup>2-</sup>, unlisted components were classified as Other.
3. The source profiles in all cases listed in the table were calculated based on the base case SGL. In the design of simulation cases, the reason why the disturbance amplitude of NH<sub>4</sub><sup>+</sup> and NO<sub>3</sub><sup>-</sup> were significantly higher than that of other components such as SO<sub>4</sub><sup>2-</sup> and Non-SNA, was because the percentages of NH<sub>4</sub><sup>+</sup> and NO<sub>3</sub><sup>-</sup> in the base source profile (SGL, based on the chemical composition of code 000002.5 in the EPA Speciate\_5.0\_0 database ) were very low, while the percentage of NH<sub>4</sub><sup>+</sup> and NO<sub>3</sub><sup>-</sup> in SPAPPC exhibited in section 2.2 were orders of magnitude higher than those in SGL.

309           Given the large number and complex chemical composition of PM<sub>2.5</sub>, it was  
310   advisable to classify them reasonably before designing sensitivity experiments. The  
311   Case DBL was to double the percentage of the listed 15 components mentioned in the  
312   above base case(SGL) (the details are shown in Fig. 4 and Table 1). As the percentage  
313   of these components increased, the proportion of unlisted components (represented by  
314   “Other”) decreased to 9% in order to meet the requirement that the total percentage of  
315   all components is 100%. Then we compared the simulation results before (SGL case)

316 and after perturbation (DBL case) in species allocation of PM<sub>2.5</sub> sources.

317 In the case DBL, when the percentage of all the components except “other” were  
318 doubled in the source profile, the simulated concentrations of Al, Ca, Cl, EC, Fe, K,  
319 Mg, Mn, Na, OC, Si and Ti doubled as well, while the simulated concentration of NO<sub>3</sub>  
320 and SO<sub>4</sub><sup>2-</sup> increased at about 3%, 10% and NH<sub>4</sub><sup>+</sup> decreased by 4%, respectively,  
321 although the simulated concentration of PM<sub>2.5</sub> was not obviously changed (Detailed  
322 simulation results were shown in Table S14). The simulation test results for SNA (SO<sub>4</sub><sup>2-</sup>,  
323 NO<sub>3</sub><sup>-</sup>, and NH<sub>4</sub><sup>+</sup>) and Non-SNA were obviously different. Therefore, we divided the  
324 components in the source profile into two groups (Non-SNA and SNA) and designed a  
325 series of sensitivity tests listed in next section to further explore how species allocation  
326 of PM<sub>2.5</sub> in emission sources affect the simulation results. The sketch of sensitivity  
327 experiment design idea was shown in Figure S7.

#### 328 4.1 Sensitivity tests design

329 Sensitivity tests were designed by changing the percentages of the target  
330 components and related components in the base case (SGL): add perturbation on each  
331 component of Non-SNA, on SO<sub>4</sub><sup>2-</sup>, on NO<sub>3</sub><sup>-</sup>, and on NH<sub>4</sub><sup>+</sup>. The general roadmap of  
332 sensitivity tests was shown in Fig. 4, and the illustration of each case was summarized  
333 in Table 1. The basic rules must be followed: a) perturbation on the percentage of each  
334 component in source profile fell within the variation range of its measured value  
335 described in section 2.2. b) The sum of the percentage of listed Non-SNA, SNA and  
336 Other components in PM<sub>2.5</sub> source profile was 100%.

#### 337 4.2 Sensitivity of simulated components to changes in source profile

338 We propose the sensitivity coefficient (δ) as evaluation index. The calculation  
339 formula is as follows:

$$340 \delta_{i,p} = \frac{\frac{C_{i\_case}}{C_{PM_{2.5\_case}}} \times 100\% - \frac{C_{i\_base}}{C_{PM_{2.5\_base}}} \times 100\%}{P_{p\_case} - P_{p\_base}} \quad (\text{For DBL and DBP, } p = i; \text{For other cases, } p = j)$$

341 ..... (2)

342 Wherein, δ<sub>i,p</sub> is the sensitivity coefficient of component *i* relative to component *p*,

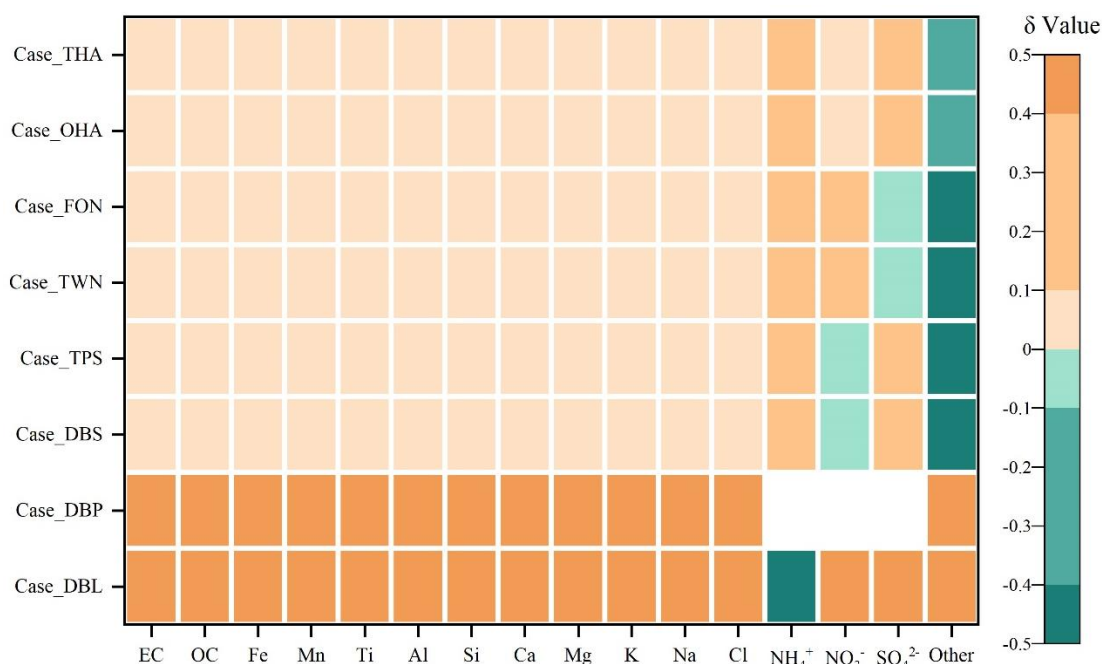
343 representing the change in simulated value of its content in ambient PM<sub>2.5</sub> corresponded  
344 to 1% perturbation in the source profiles.  $C_{i\_case}$  is the simulated concentration of  
345 component  $i$  in each sensitivity experiment case,  $\mu\text{g}/\text{m}^3$ ;  $C_{i\_base}$  is the simulated  
346 concentration of components  $i$  in base case,  $\mu\text{g}/\text{m}^3$ ;  $C_{PM_{2.5}\_case}$  is the simulated  
347 concentration of PM<sub>2.5</sub> in each sensitivity experiment case,  $\mu\text{g}/\text{m}^3$ ;  $C_{PM_{2.5}\_base}$  is the  
348 simulated concentration of PM<sub>2.5</sub> in base case,  $\mu\text{g}/\text{m}^3$ ;  $P_{p\_case}$  is the percentage of  
349 component  $p$  in source profile of sensitivity experiment case, %;  $j$  is the perturbed  
350 component  $j$  in different source profile of sensitivity experiment cases;  $P_{p\_base}$  is the  
351 percentage of component  $p$  in source profile of base case, %.

352 The positive value of  $\delta$  means the simulated concentration of PM<sub>2.5</sub> component  
353 increases (decreases) with the increase (decrease) of perturbation on the percentage of  
354 components in source profile, negative  $\delta$  is just the opposite. If the absolute value of  $\delta$   
355 is less than or equal to 0.1, the simulated component is considered to be insensitive to  
356 the corresponding variation of source profile; If the absolute value of  $\delta$  falls between  
357 0.1 and 0.4 (included), the simulated component is considered to be sensitive to the  
358 variation of source profile; If the absolute value of  $\delta$  is larger than 0.4, the simulated  
359 component is very sensitive to the variation of source profile. The greater the absolute  
360 value of  $\delta$  is, indicates the variation of source profile adopted in CMAQ has more  
361 obvious impact on the simulated results of PM<sub>2.5</sub> chemical components.

362 Fig.5 listed the sensitivity coefficients of simulated ambient PM<sub>2.5</sub> components to  
363 the perturbation of source profile under each test case. In case DBL (doubled the  
364 percentage of the listed components in the source profile of base case and decreased the  
365 proportion of unlisted other components to 9%), the sensitivity coefficient ( $\delta$ ) of  $\text{NH}_4^+$   
366 was negative, and the absolute value was high, indicating that the simulated proportion  
367 of  $\text{NH}_4^+$  in ambient PM<sub>2.5</sub> decreased, and it was very sensitive to the variation of source  
368 profile. Conversely, the sensitivity coefficient of  $\text{NO}_3^-$  was close to 1, which illustrated  
369 that the simulated proportion of  $\text{NO}_3^-$  in ambient PM<sub>2.5</sub> increased proportionally with  
370 the change in source profile. The simulated  $\text{SO}_4^{2-}$  also showed a very sensitive property.



371 The simulated Non-SNA concentrations were doubled when compared to the base case  
 372 (SGL).



373  
 374 Fig. 5 The sensitivity coefficients ( $\delta$ ) of simulated components to the perturbation of adopted source  
 375 profile in different cases. Note: Each small color box in the figure represented the sensitivity level  
 376 (indicated by the legend on the right) of PM<sub>2.5</sub> components (the x-coordinate) in different cases (y-  
 377 coordinate). The blank grids in DBP case indicated no perturbation to SNA in PM<sub>2.5</sub> source profile  
 378 under this case.

379 In case DBP, when the percentages of listed Non-SNA (Al, Ca, Cl, EC, Fe, K, Mg,  
 380 Mn, Na, OC, Si and Ti) in the source profile were doubled, the simulated proportions  
 381 of Non-SNA in ambient PM<sub>2.5</sub> synchronous increased, and were very sensitive to the  
 382 change in the adopted source profile with a sensitivity coefficient ( $\delta$ ) of 0.5.  
 383 Interestingly, the simulated concentration of SNA in ambient PM<sub>2.5</sub> also changed  
 384 although the SNA in source profile did not change, the concentration of NO<sub>3</sub><sup>-</sup> and SO<sub>4</sub><sup>2-</sup>  
 385 increased by 2% and 3%, respectively, NH<sub>4</sub><sup>+</sup> decreased by 10% (Detail simulation  
 386 results of each case were shown on Table S15~S21).

387 Under SO<sub>4</sub><sup>2-</sup> perturbation cases (Case DBS and Case TPS), we found the simulated  
 388 results of Non-SNA and NO<sub>3</sub><sup>-</sup> had no obvious variation compared with the base case.  
 389 Either in Case DBS or in Case TPS, the  $\delta$  of Non-SNA and NO<sub>3</sub><sup>-</sup> were between -0.1 to  
 390 0.1. But when the percentage of SO<sub>4</sub><sup>2-</sup> was doubled in source profile (DBS), the

391 simulated concentration of  $\text{NH}_4^+$  and  $\text{SO}_4^{2-}$  increased by 6% and 8%, respectively. In  
392 Case TPS (the percentage of  $\text{SO}_4^{2-}$  was tripled), the simulated concentration of  $\text{NH}_4^+$   
393 and  $\text{SO}_4^{2-}$  were increased by 11% and 16%, respectively. The  $\delta$  of  $\text{NH}_4^+$  and  $\text{SO}_4^{2-}$  were  
394 0.12 and 0.36, sensitive toward to positive direction with the increase of  $\text{SO}_4^{2-}$  in the  
395 source profile.

396 In the situation of  $\text{NO}_3^-$  perturbation in source profile (Case TWN and Case FON),  
397 the simulated Non-SNA hardly change when compared to the base case, while changing  
398 patterns of simulated SNA were different. The simulation concentration of  $\text{NH}_4^+$   
399 increased by 2.6% and 5.4% compared with the base case, the simulated  $\text{NO}_3^-$  increased  
400 by 14% and 30%, the simulated  $\text{SO}_4^{2-}$  decreased slightly, even could be neglected in  
401 some observation sites. The simulated concentrations of Non-SNA and  $\text{SO}_4^{2-}$  were  
402 insensitive to the perturbation of  $\text{NO}_3^-$  in source profile;  $\text{NH}_4^+$  was sensitive, and  $\text{NO}_3^-$   
403 was very sensitive.

404 When we put perturbation on  $\text{NH}_4^+$  in the source profile (Case OHA and Case  
405 THA), the simulation results of Non-SNA were almost not changed, the simulated  
406 concentration of  $\text{SO}_4^{2-}$ ,  $\text{NH}_4^+$ ,  $\text{NO}_3^-$  increased. The  $\delta$  of SNA to the variation of  $\text{NH}_4^+$  in  
407 the source profile were positive and  $\delta_{\text{SO}_4^{2-}, \text{NH}_4^+} > \delta_{\text{NH}_4^+, \text{NH}_4^+} > \delta_{\text{NO}_3^-, \text{NH}_4^+}$ ,  $\text{SO}_4^{2-}$  and  $\text{NH}_4^+$   
408 were sensitive to the  $\text{NH}_4^+$  perturbation in the source profile, but  $\text{NO}_3^-$  was not so  
409 sensitive.

410 In general, the simulation results of components in ambient  $\text{PM}_{2.5}$  were affected in  
411 one way or another by the change of source profiles adopted by CMAQ. Both of the  
412 simulated Non-SNA and SNA were very sensitive to the perturbation of Non-SNA in  
413 source profile. When the percentage of SNA changed in the source profile, simulated  
414 Non-SNA generally have little change, but the simulation results of SNA could change  
415 in different patterns: the simulated  $\text{SO}_4^{2-}$  was very sensitive and  $\text{NH}_4^+$  was sensitive to  
416 the perturbation of  $\text{SO}_4^{2-}$  in source profile; simulated  $\text{NO}_3^-$  was very sensitive and  $\text{NH}_4^+$   
417 was sensitive to the perturbation of  $\text{NO}_3^-$  in source profile;  $\text{SO}_4^{2-}$  and  $\text{NH}_4^+$  were  
418 sensitive to the perturbation of  $\text{NH}_4^+$  in source profile. The simulated component such  
419 as  $\text{SO}_4^{2-}$  was influenced not only by the change of  $\text{SO}_4^{2-}$  itself but also by other

420 components like some Non-SNA and  $\text{NH}_4^+$  in the source profile. In other words, there  
 421 was a linkage effect, variation of some components in the source profile would bring  
 422 changes to the simulated results of other components.

423 **5 How does the impact work?**

424 The variation of species allocation in emission sources can directly affect the  
 425 composition of aerosol system in CTMs. In CMAQv5.0.2, the aerosol thermodynamic  
 426 equilibrium process is carried out according to ISORROPIA II, including a  $\text{SO}_4^{2-}$ - $\text{NO}_3^-$ -  
 427  $\text{Cl}^-$ - $\text{NH}_4^+$ - $\text{Na}^+$ - $\text{K}^+$ - $\text{Mg}^{2+}$ - $\text{Ca}^{2+}$ - $\text{H}_2\text{O}$  system (Detailed equilibrium relations were shown  
 428 in Table S22). Some assumptions have been made in the ISORROPIA model to simplify  
 429 the simulation system (Fountoukis and Nenes, 2007): (1) Because the vapor pressure  
 430 of sulfuric acid and metal salts (such as  $\text{Na}^+$ ,  $\text{Ca}^{2+}$ ,  $\text{K}^+$ ,  $\text{Mg}^{2+}$ ) are very low, it is assumed  
 431 that all the sulfuric acid and metal salts in the system existed in the aerosol phase; (2)  
 432 For ammonia in the system, it is preferred to have an irreversible reaction with sulfuric  
 433 acid to produce ammonium sulfate. Only when there is still surplus  $\text{NH}_3$  after the  
 434 neutralization of  $\text{H}_2\text{SO}_4$ , can it have a reversible reaction with  $\text{HNO}_3$  and  $\text{HCl}$  to  
 435 produce  $\text{NH}_4\text{NO}_3$  and  $\text{NH}_4\text{Cl}$ . (3) For sulfuric acid in the system, if there are metal ions  
 436 (such as  $\text{Ca}^{2+}$ ,  $\text{Mg}^{2+}$ ,  $\text{K}^+$ ,  $\text{Na}^+$ ) in the system, sulfuric acid would react with metal ions  
 437 to produce metal salts. Only in the case of insufficient sodium, sulfuric acid would react  
 438 with ammonia. Based on these assumptions, the ISORROPIA model introduces the  
 439 following three judgment parameters ( $R_1$ ,  $R_2$  and  $R_3$ ) to determine the simulation  
 440 subsystems, these parameters are calculated by the following formulas:

441 
$$R_1 = \frac{[\text{NH}_4^+] + [\text{Ca}^{2+}] + [\text{K}^+] + [\text{Mg}^{2+}] + [\text{Na}^+]}{[\text{SO}_4^{2-}]} \dots\dots\dots (3)$$

442 
$$R_2 = \frac{[\text{Ca}^{2+}] + [\text{K}^+] + [\text{Mg}^{2+}] + [\text{Na}^+]}{[\text{SO}_4^{2-}]} \dots\dots\dots (4)$$

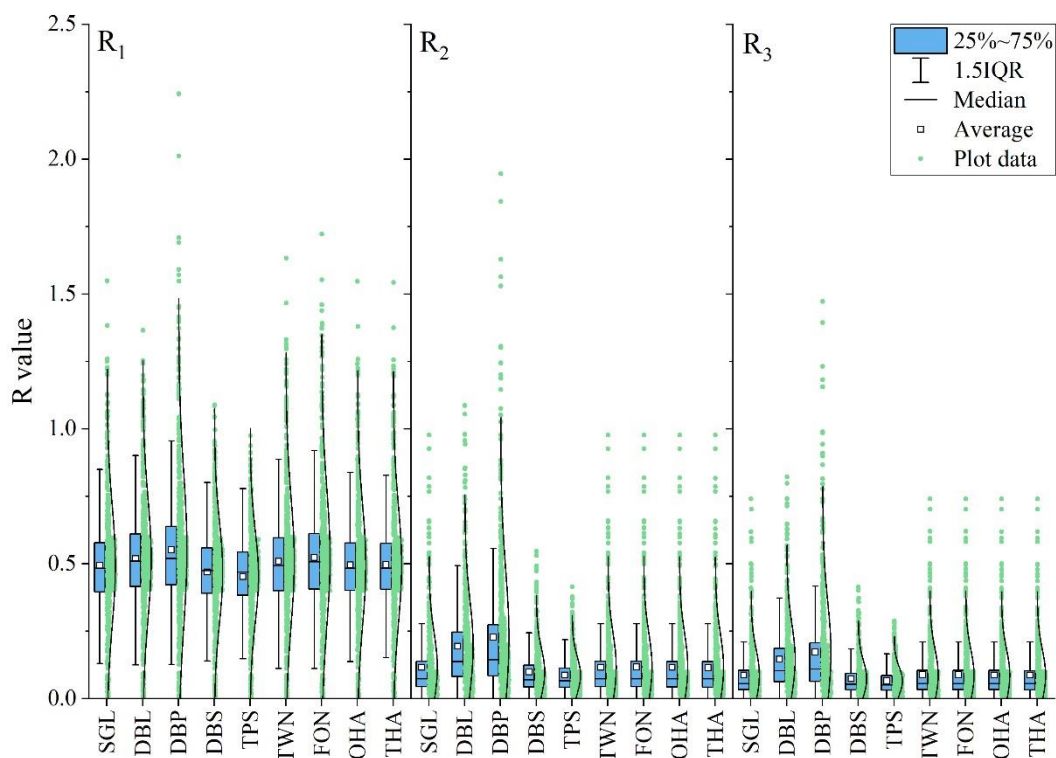
443 
$$R_3 = \frac{[\text{Ca}^{2+}] + [\text{K}^+] + [\text{Mg}^{2+}]}{[\text{SO}_4^{2-}]} \dots\dots\dots (5)$$

444 Where  $[X]$  denotes molar concentration of component ( $\text{mol}\cdot\text{m}^{-3}$ ),  $R_1$ ,  $R_2$  and  $R_3$

445 are termed as “total sulfate ratio”, “crustal species and sodium ratio” and “crustal  
 446 species ratio” respectively; The number of species and equilibrium reactions are  
 447 determined by the relative abundance of NH<sub>3</sub>, Na, Ca, K, Mg, HNO<sub>3</sub>, HCl, H<sub>2</sub>SO<sub>4</sub>, as  
 448 well as the ambient relative humidity and temperature. Guide by the value of R<sub>1</sub>, R<sub>2</sub> and  
 449 R<sub>3</sub>, 5 aerosol composition regimes in ISORROPIA are defined. (Detail rules are shown  
 450 in Table S27 and solving procedure in Figure S8). R<sub>1</sub>, R<sub>2</sub> and R<sub>3</sub> under each sensitivity  
 451 test case were shown in Fig. 6. These components achieved thermodynamic equilibrium  
 452 in the order of preference for more stable salts, obviously, the simulation processes of  
 453 these components may influence each other.

### 454 5.1 General results

455 Our sensitivity experiment focuses on examining the impact of source profile  
 456 changes on simulated PM<sub>2.5</sub> components. For given meteorological conditions, we  
 457 analyze the sensitivity of simulated components to variations in the source chemical  
 458 profile by comparing the simulation results between perturbed cases and base case.



459

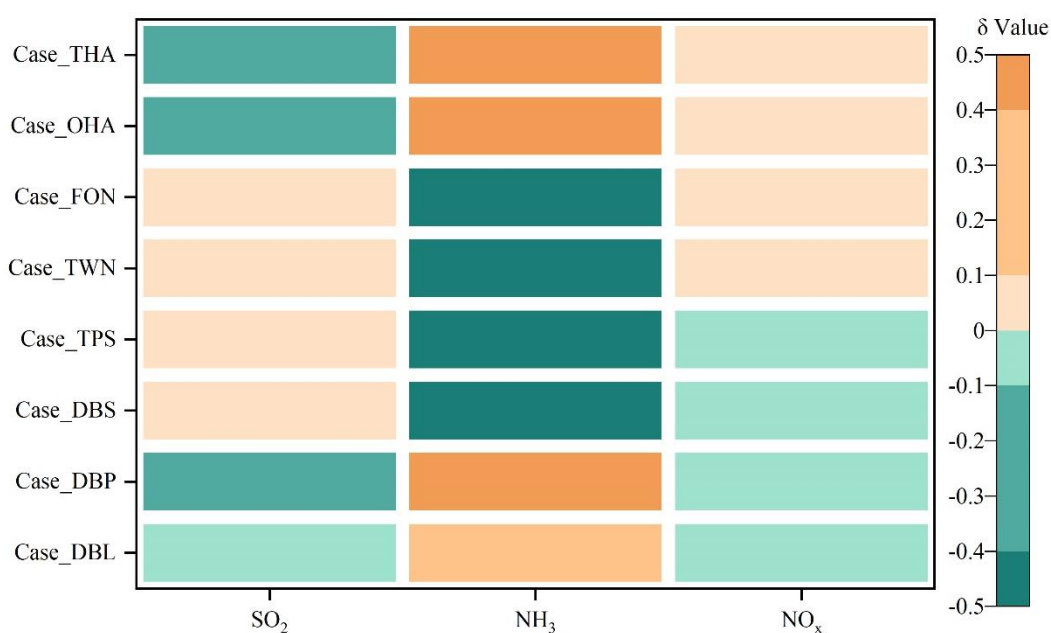
460

Fig. 6 R values' distribution of among base case and different sensitivity test cases

461

In Non-SNA perturbation case, when the percentage of Non-SNA in source profile

462 doubled (Case DBP), meant there were more Na, K, Mg, Ca, Cl participated in aerosol  
 463 chemistry, the model system needed more  $\text{SO}_4^{2-}$  and  $\text{NO}_3^-$  on the basis of charge balance  
 464 and the thermodynamic equilibrium shifted to the direction of consuming Ca Mg, K  
 465 and Na, which resulted in the increase of the simulated concentration of  $\text{SO}_4^{2-}$  and  $\text{NO}_3^-$ .  
 466 Meanwhile, according to the rule of anions preferentially binding with nonvolatile  
 467 cations in ISORROPIA, the increased cations  $\text{Na}^+$ ,  $\text{K}^+$ ,  $\text{Mg}^{2+}$ ,  $\text{Ca}^{2+}$  directly led to  
 468 the decrease of anions binding with  $\text{NH}_4^+$ , there were less reaction dose between  $\text{SO}_4^{2-}$   
 469 and  $\text{NH}_4^+$  to form  $(\text{NH}_4)_2\text{SO}_4$  or  $\text{NH}_4\text{HSO}_4$ , ultimately resulted in a decrease in  
 470 simulated concentration of  $\text{NH}_4^+$  compared with the base case. Because in this case  
 471 more anions such as  $\text{SO}_4^{2-}$  were passively needed, according to the principle of chemical  
 472 equilibrium mentioned above, the chemical conversion of  $\text{SO}_2$  to  $\text{SO}_4^{2-}$  was promoted,  
 473 the simulated secondary  $\text{SO}_4^{2-}$  increased, this could be proved by that the sensitivity  
 474 coefficient  $\delta$  of  $\text{SO}_2$  in Case DBP was negative (shown in Fig. 7, details of other  
 475 monitoring stations' results were shown Table S25).



476  
 477 Fig.7 The sensitivity coefficients ( $\delta$ ) of simulated gas pollutants to the change of adopted source  
 478 profile in different cases.

479 Similarly, with the increase of metal ions in the system to bond with anions, the  
 480 number of anions which can bind to  $\text{NH}_4^+$  decreased. The system needed less  $\text{NH}_4^+$  and  
 481 weakened the need for conversion from  $\text{NH}_3$  to  $\text{NH}_4^+$ , the simulated  $\text{NH}_4^+$  concentration

482 decreased while the  $\delta$  of  $\text{NH}_3$  was positive and very sensitive. Different trends of  
483 simulated concentration of gaseous pollutants mirrored the rules mentioned above from  
484 another aspect. The  $\delta$  of  $\text{SO}_2$  and  $\text{NO}_x$  was negative,  $\text{NH}_3$  was positive. We could see  
485 the same phenomena in DBL case (Fig. 7). When the percentages of Non-SNA in source  
486 profile increased, they not only affected the simulated concentration of Non-SNA, but  
487 also the secondary  $\text{SO}_4^{2-}$ ,  $\text{NO}_3^-$  and  $\text{NH}_4^+$ .

488 In  $\text{SO}_4^{2-}$  perturbation cases (Case DBS and TPS), as the percentage of  $\text{SO}_4^{2-}$  in  
489 source profile increased, for the chemical reactions of sulfate radical consuming (as  
490 shown in Table S22), the chemical equilibrium would move toward the products  
491 compared with the base case. While for the chemical reactions of sulfate radical  
492 formation (The equations were shown in Table S23), meant the product was added in,  
493 the chemical equilibrium would be pushed toward the reactants. The chemical reactions  
494 between  $\text{SO}_4^{2-}$  and  $\text{NH}_4^+$  would shift to the direction of  $(\text{NH}_4)_2\text{SO}_4$  or  $\text{NH}_4\text{HSO}_4$   
495 generation, we could see the simulated concentrations of  $\text{NH}_4^+$  in DBS and TPS were  
496 both higher and  $\text{NH}_3$  were lower than those in the base case (SGL). In addition, when  
497 more  $\text{SO}_4^{2-}$  was added in the system, the conversion of  $\text{SO}_2$  to  $\text{SO}_4^{2-}$  was affected in  
498 some level and consumed less  $\text{SO}_2$  than the base case, simulated  $\text{SO}_2$  showed insensitive  
499 but positive trend (Fig.7). And the potential solid phase species in ISORROPIA II under  
500 DBS and TPS cases (shown in Table S27) were mainly consisted of sulfate salts, so the  
501 simulated concentration of  $\text{NO}_3^-$  did not change apparently.

502 As the percentage of  $\text{NO}_3^-$  in source profile increased (Case FON and TWN), the  
503 associated chemical equilibrium shifted towards the consumption of  $\text{NO}_3^-$ , such as  $\text{NH}_4^+$   
504 +  $\text{NO}_3^- \rightarrow \text{NH}_4\text{NO}_3$ , which would also consume more  $\text{NH}_4^+$  and form more ammonium  
505 salt, finally consumed more  $\text{NH}_3$  because of  $\text{NH}_3(\text{gas}) + \text{H}_2\text{O}(\text{aq}) \rightarrow \text{NH}_4^+(\text{aq}) + \text{OH}^-$   
506 (aq). The simulation results also manifested that the concentration of  $\text{NH}_4^+$  increased  
507 while that of  $\text{NH}_3$  decreased. Based on the assumption of ISORROPIA, the cations like  
508  $\text{Na}^+$ ,  $\text{K}^+$ ,  $\text{Mg}^{2+}$ ,  $\text{Ca}^{2+}$  and  $\text{NH}_4^+$  preferentially to react with  $\text{SO}_4^{2-}$ , only if there were  
509 cations left after neutralized  $\text{SO}_4^{2-}$ , could they react with  $\text{NO}_3^-$  to form salts, so the  
510 simulated concentration of  $\text{SO}_4^{2-}$  was not obviously changed. Accordingly, the

511 simulated concentration of NO<sub>x</sub> and SO<sub>2</sub> almost unchanged (The δ of NO<sub>x</sub> and SO<sub>2</sub>  
512 displayed insensitive).

513 In the cases of NH<sub>4</sub><sup>+</sup> perturbation (Case OHA and THA), when the percentage of  
514 NH<sub>4</sub><sup>+</sup> in source profile increased, the related chemical equilibrium shifted towards the  
515 direction of NH<sub>4</sub><sup>+</sup> consumption, such as in 2NH<sub>4</sub><sup>+</sup> +SO<sub>4</sub><sup>2-</sup> → (NH<sub>4</sub>)<sub>2</sub>SO<sub>4</sub> or NH<sub>4</sub><sup>+</sup>+H<sup>+</sup>,  
516 SO<sub>4</sub><sup>2-</sup> → NH<sub>4</sub>HSO<sub>4</sub>, more SO<sub>4</sub><sup>2-</sup> was consumed at the same time, which further  
517 promoted the conversion of SO<sub>2</sub> to SO<sub>4</sub><sup>2-</sup>. The increased NH<sub>4</sub><sup>+</sup> in OHA and THA also  
518 would inhibit the conversion of NH<sub>3</sub> to NH<sub>4</sub><sup>+</sup> compared with the base case. This, in turn  
519 appeared as the increase of the simulated secondary SO<sub>4</sub><sup>2-</sup> and NH<sub>3</sub>, and the decrease  
520 of the simulated SO<sub>2</sub>.

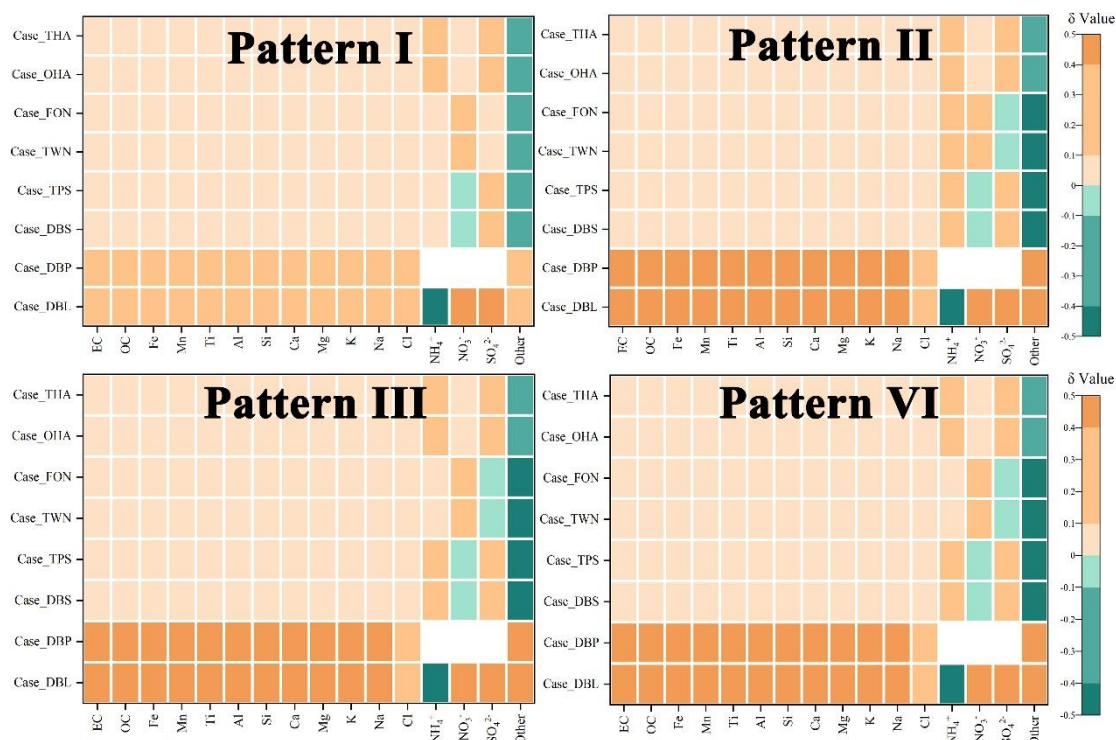
## 521 **5.2 Results from stratified analysis**

522 For each case, the distribution of R values was related to meteorological conditions  
523 (as shown in Fig. 6). To illustrate the role of meteorological conditions in the  
524 mechanism of how source profile affected the simulated PM<sub>2.5</sub> components, stratified  
525 analysis was used. The hourly simulation result of temperature and humidity (affecting  
526 ISORROPIA solving procedure), wind field (affecting flux in and flux out for each grid)  
527 were incorporate into K-means clustering. When the number of clusters was equal to or  
528 greater than 4, there was a significant inflection point between data points and their  
529 assigned cluster centroids (Figure S9). Hence, 4 patterns of meteorological conditions  
530 were selected to the subsequent analysis.

531 For pattern I, II, III and IV, as shown in Fig. 8, the rule similar to the general result  
532 was observed. From a global view, the subdivisional (category-specific) sensitivity of  
533 simulated PM<sub>2.5</sub> components to source chemical profile under different patterns are  
534 similar; From a local perspective, their sensitivity levels are slightly different; For  
535 example, in pattern II, the simulated NH<sub>4</sub><sup>+</sup> was very sensitive to the perturbation of  
536 SO<sub>4</sub><sup>2-</sup>; While in pattern I, III and VI was sensitive, but it remained the major component  
537 that underwent change (These results were also shown in Table S28 of supplementary  
538 material).

539 When we perturb source profile, some species/reactants increase (or reduce) in the

540 system, the chemical equilibrium shift to the direction of consuming more (or less)  
 541 reactants, as shown in Figure S10. Under different patterns of meteorological conditions  
 542 (determining the values of R), the influence pathways of chemical source profile  
 543 changes on the simulated PM<sub>2.5</sub> components have the same laws with general results.



544  
 545 Fig. 8 The sensitivity coefficients ( $\delta$ ) under different hierarchical patterns

546 In summary, the effects of source profile variation on the simulation results of  
 547 different components were linked. When the percentages of Non-SNA, SO<sub>4</sub><sup>2-</sup>, NO<sub>3</sub><sup>-</sup> and  
 548 NH<sub>4</sub><sup>+</sup> in the source profile changed, they not only affected the simulated concentration  
 549 of themselves, but also affected the simulation results of some other components. Both  
 550 the simulation results of primary components and secondary components were affected  
 551 by the change of source profile, the secondary SO<sub>4</sub><sup>2-</sup> and NH<sub>4</sub><sup>+</sup> were affected more than  
 552 the secondary NO<sub>3</sub><sup>-</sup>.

## 553 6 Conclusions

554 The influence of source profile variation on the simulated PM<sub>2.5</sub> components  
 555 cannot be ignored, as simulation results of some components are sensitive to the  
 556 adopted source profile in CTMs, e.g., both the simulated Non-SNA and SNA are



557 sensitive to the perturbation of Non-SNA in source profile, the simulated  $\text{SO}_4^{2-}$  and  
558  $\text{NH}_4^+$  are sensitive to the perturbation of  $\text{SO}_4^{2-}$ , simulated  $\text{NO}_3^-$  and  $\text{NH}_4^+$  are sensitive  
559 to the perturbation of  $\text{NO}_3^-$ ,  $\text{SO}_4^{2-}$  and  $\text{NH}_4^+$  are sensitive to the perturbation of  $\text{NH}_4^+$ .  
560 These influences are not only specific to an individual component, but also can be  
561 transmitted and linked among components. The influence path is connected to chemical  
562 mechanisms in the model since the variation of species allocation in emission sources  
563 directly affect the thermodynamic equilibrium system (ISORROPIA II,  $\text{SO}_4^{2-}$ - $\text{NO}_3^-$ - $\text{Cl}^-$   
564 - $\text{NH}_4^+$ - $\text{Na}^+$ - $\text{K}^+$ - $\text{Mg}^{2+}$ - $\text{Ca}^{2+}$ - $\text{H}_2\text{O}$  system).

565 It is generally believed that changes in source profile would have an impact on the  
566 simulation result of primary  $\text{PM}_{2.5}$ , but interestingly, the simulation of secondary  
567 components could be affected as well. We found the perturbation of  $\text{PM}_{2.5}$  source profile  
568 caused the variation of simulation results of gaseous pollutants by influencing related  
569 chemical reactions like gas-phase chemistry of  $\text{SO}_2$ ,  $\text{NO}_x$  and  $\text{NH}_3$ . Overall, the  
570 emission source profile used in CTMs is one of the important factors affecting the  
571 simulation results of  $\text{PM}_{2.5}$  chemical components. Additionally, organic species are one  
572 of the most important components in  $\text{PM}_{2.5}$  and gain much more attention on human  
573 health. While the number of organic species in source profile is relatively scarce which  
574 brings a challenge for simulation test designing, the influence of source profile on the  
575 simulation results of organic species is not taken into account in this study.

576 With the change of fuel and raw materials, the development of production  
577 technology and the innovation of pollution treatment technology in recent years, some  
578 components have changed significantly in source profiles. Given the important role of  
579 air quality simulation in decision making for pollution control and health risk  
580 assessment, the representativeness and timeliness of the source profile should be  
581 considered.

582 Our study tentatively discussed the influence mechanism of  $\text{PM}_{2.5}$  emission source  
583 profiles on the simulation results of components in CTMs. The size distribution, mixing  
584 state, aging and solubility for different aerosol components might have something to do  
585 with source profile, how much the influence of source profile changes on the simulation

586 of these physical and chemical process, is deserved to do in the future.

### 587 **Data availability**

588 The input datasets for WRF simulation are available at  
589 <https://doi.org/10.5065/D6M043C6> (The National Center for Atmospheric Research  
590 (NCAR)). The PM<sub>2.5</sub> emission source profiles from database of Source Profiles of Air  
591 Pollution (SPAP) (<http://www.nkspap.com:9091/>, Nankai university), SPECIATE  
592 database (<https://www.epa.gov/air-emissions-modeling/speciate>, U.S. Environmental  
593 Protection Agency's (EPA)), Mendeley data repository  
594 (<https://doi.org/10.17632/x8dfshjt9j.2>, Bi et al., 2019). Tutorial guide for accessing  
595 Database of Source Profiles of Air Pollution (SPAP), input and output data, emission  
596 data repository (<https://zenodo.org/record/7865675>).

### 597 **Code availability**

598 The source code for CMAQ version 5.0.2 is available at  
599 <https://github.com/USEPA/CMAQ/tree/5.0.2> (last access: April 2014)  
600 (<https://doi.org/10.5281/zenodo.1079898>, US EPA Office of Research and  
601 Development, 2018). The source code for WRF version 3.7.1 is available at  
602 <https://www2.mmm.ucar.edu/wrf/src/WRFV3.7.1.TAR.gz>.

### 603 **Author contributions**

604 Zhongwei Luo: Data curation and collection, writing–original draft. Yan Han:  
605 Modeling, writing–original draft. Kun Hua: Data collection. Yufen Zhang:  
606 Supervision–Review & editing. Jianhui Wu: Supervision in source profile. Xiaohui Bi:  
607 Supervision in source profile. Qili Dai: Resources. Baoshuang Liu: Resources. Yang  
608 Chen: Modification and editing. Xin Long: Supervision in modeling. Yinchang Feng:  
609 Supervision–Review & editing.

### 610 **Competing interests**

611 The authors declare that they have no known competing financial interests or

612 personal relationships that could have appeared to influence the work reported in this  
613 paper.

#### 614 **Disclaimer. Publisher's note**

615 Copernicus Publications remains neutral with regard to jurisdictional claims in  
616 published maps and institutional affiliations.

#### 617 **Acknowledgements**

618 We would like to thank the National Natural Science Foundation of China (grant  
619 number 42177465) for providing funding for the project. We are grateful for the  
620 Inventory Spatial Allocate Tool (ISAT) provided by Kun Wang from Department of Air  
621 Pollution Control, Institute of Urban Safety and Environmental Science, Beijing  
622 Academy of Science and Technology. We thank Klaus Klingmüller (Top Editor), Astrid  
623 Kerkweg (Executive Editor) and three anonymous referees for the time and effort spent  
624 in reviewing the manuscript. And also thank Polina Shvedko, Sarah Schneemann, Sarah  
625 Buchmann for the suggestions and assistance.

#### 626 **Financial support**

627 This study was financially supported by the National Natural Science Foundation  
628 of China (grant number 42177465).

#### 629 **Reference**

- 630 Appel, K. W., Poullo, G. A., Simon, H., Sarwar, G., Pye, H. O. T., Napelenok, S. L., Akhtar, F.,  
631 Roselle, S. J.: Evaluation of dust and trace metal estimates from the Community Multiscale Air  
632 Quality (CMAQ) model version 5.0, *Geosci. Model Dev.*, 6, 883-899,  
633 <https://doi.org/10.5194/gmd-6-883-2013>, 2013.
- 634 Bi, X., Dai, Q., Wu, J., Zhang, Q., Zhang, W., Luo, R., Cheng, Y., Zhang, J., Wang, L., Yu, Z., Zhang,  
635 Y., Tian, Y., Feng, Y.: Characteristics of the main primary source profiles of particulate matter  
636 across China from 1987 to 2017, *Atmos. Chem. Phys.*, 19, 3223-3243,  
637 <https://doi.org/10.5194/acp-19-3223-2019>, 2019.
- 638 Cao, J., Qiu, X., Gao, J., Wang, F., Wang, J., Wu, J., Peng, L.: Significant decrease in SO<sub>2</sub> emission  
639 and enhanced atmospheric oxidation trigger changes in sulfate formation pathways in China  
640 during 2008–2016, *J. Clean. Prod.*, 326, 129396, <https://doi.org/10.1016/j.jclepro.2021.129396>,  
641 2021.
- 642 Chapel Hill, N.: Operational Guidance for the Community Multiscale Air Quality (CMAQ)

643 Modeling System Version 5.0, [https://www.airqualitymodeling.org/index.php/CMAQ\\_ vers](https://www.airqualitymodeling.org/index.php/CMAQ_version_5.0_(February_2010_release)_OGD#Aerosol_Module)  
644 [ion\\_5.0 \(February 2010 release\) OGD#Aerosol Module](https://www.airqualitymodeling.org/index.php/CMAQ_version_5.0_(February_2010_release)_OGD#Aerosol_Module), last access: February 2012.

645 Chen, Z., Chen, D., Zhao, C., Kwan, M., Cai, J., Zhuang, Y., Zhao, B., Wang, X., Chen, B., Yang,  
646 J., Li, R., He, B., Gao, B., Wang, K., Xu, B.: Influence of meteorological conditions on PM<sub>2.5</sub>  
647 concentrations across China: A review of methodology and mechanism, *Environ. Int.*, 139,  
648 105558, <https://doi.org/10.1016/j.envint.2020.105558>, 2020.

649 Cheng, N. L., Meng, F., Wang, J. K., Chen, Y. B., Wei, X., Han, H.: Numerical simulation of the  
650 spatial distribution and deposition of PM<sub>2.5</sub> in East China coastal area in 2010 (In Chinese),  
651 *Journ. Safety Environ.*, 15, 305-310, <https://doi.org/10.13637/j.issn.1009-6094.2015.06.063>,  
652 2015.

653 Eder, B. K., Yu, S. C.: A performance evaluation of the 2004 release of Models-3 CMAQ, *Atmos.*  
654 *Environ.*, 40, 4811-4824, [http://doi.org/10.1007/978-0-387-68854-1\\_57](http://doi.org/10.1007/978-0-387-68854-1_57), 2006.

655 Foley, K. M., Roselle, S. J., Appel, K. W., Bhave, P. V., Pleim, J., Otte, T., Mathur, R., Sarwar, G.,  
656 Young, J. O., Gilliam, R.: Incremental testing of the community multiscale air quality (CMAQ)  
657 modeling system version 4.7, *Geosci. Model Dev.*, 3, 205-226, [https://doi.org/10.5194/gmd-3-](https://doi.org/10.5194/gmd-3-205-2010)  
658 [205-2010](https://doi.org/10.5194/gmd-3-205-2010), 2010.

659 Fountoukis, C., Nenes, A.: ISORROPIA II: a computationally efficient thermodynamic equilibrium  
660 model for K<sup>+</sup>-Ca<sup>2+</sup>-Mg<sup>2+</sup>-NH<sub>4</sub><sup>+</sup>-Na<sup>+</sup>-SO<sub>4</sub><sup>2-</sup>-NO<sub>3</sub><sup>-</sup>-Cl<sup>-</sup>-H<sub>2</sub>O aerosols, *Atmos. Chem. Phys.*, 7,  
661 4639-4659, <https://doi.org/10.5194/acp-7-4639-2007>, 2007.

662 Fu, X., Wang, S., Zhao, B., Xing, J., Cheng, Z., Liu, H., Hao, J.: Emission inventory of primary  
663 pollutants and chemical speciation in 2010 for the Yangtze River Delta region, China, *Atmos.*  
664 *Environ.*, 70, 39-50, <https://doi.org/10.1016/j.atmosenv.2012.12.034>, 2013.

665 Fu, X., Wang, S. X., Chang, X., Cai, S., Xing, J., Hao, J. M.: Modeling analysis of secondary  
666 inorganic aerosols over China: pollution characteristics, and meteorological and dust impacts,  
667 *Sci. Rep.*, 6, 35992, <https://doi.org/10.1038/srep35992>, 2016.

668 Gao, S., Zhang, S., Che, X., Ma, Y., Chen, X., Duan, Y., Fu, Q., Wang, S., Zhou, B., Wei, C., Jiao,  
669 Z.: New understanding of source profiles: Example of the coating industry, *J. Clean. Prod.*, 357,  
670 132025, <https://doi.org/10.1016/j.jclepro.2022.132025>, 2022.

671 Guo, R., Yang, J., Liu, Z.: Influence of heat treatment conditions on release of chlorine from Datong  
672 coal, *J. Anal. Appl. Pyrol.*, 71, 179-186, [https://doi.org/10.1016/S0165-2370\(03\)00086-X](https://doi.org/10.1016/S0165-2370(03)00086-X),  
673 2004.

674 Guo, Y. Y., Gao, X., Zhu, T. Y., Luo, L., Zheng, Y.: Chemical profiles of PM emitted from the iron  
675 and steel industry in northern China, *Atmos. Environ.*, 150, 187-197,  
676 <https://doi.org/10.1016/j.atmosenv.2016.11.055>, 2017.

677 Guo, Z., Hao, Y., Tian, H., Bai, X., Wu, B., Liu, S., Luo, L., Liu, W., Zhao, S., Lin, S., Lv, Y., Yang,  
678 J., Xiao, Y.: Field measurements on emission characteristics, chemical profiles, and emission  
679 factors of size-segregated PM from cement plants in China, *Sci. Total Environ.*, 151822,  
680 <https://doi.org/10.1016/j.scitotenv.2021.151822>, 2021.

681 Han, Y., Xu, H., Bi, X. H., Lin, F. M., Li, J., Zhang, Y. F., Feng, Y. C.: The effect of atmospheric  
682 particulates on the rainwater chemistry in the Yangtze River Delta, China, *J. Air Waste Manage.*,  
683 69, 1452-1466, <https://doi.org/10.1080/10962247.2019.1674750>, 2019.

684 Hopke, P. K., Dai, Q., Li, L., Feng, Y.: Global review of recent source apportionments for airborne  
685 particulate matter, *Sci. Total Environ.*, 740, 140091,  
686 <https://doi.org/10.1016/j.scitotenv.2020.140091>, 2020.

687 Hopke, P. K., Feng, Y. C., Dai, Q.: Source apportionment of particle number concentrations: A global  
688 review, *Sci. Total Environ.*, 819, 153104, <https://doi.org/10.1016/j.scitotenv.2022.153104>,  
689 2022.

690 Hsu, Y., Divita, F., Dorn, J.: SPECIATE 5.0 - Speciation Database Development Documentation,  
691 Final Report, M. MENETREZ, Abt Associates Inc./Office of Research and Development/U.S.  
692 Environmental Protection Agency Research Triangle Park, NC27711,  
693 [https://www.epa.gov/sites/default/files/2019-07/documents/speciate\\_5.0.pdf](https://www.epa.gov/sites/default/files/2019-07/documents/speciate_5.0.pdf), 2019.

694 Huang, C. H., Hu, J. L., Xue, T., Xu, H., Wang, M.: High-Resolution Spatiotemporal Modeling for  
695 Ambient PM<sub>2.5</sub> Exposure Assessment in China from 2013 to 2019, *Environ. Sci. Technol.*, 55,  
696 2152-2162, <https://doi.org/10.1021/acs.est.0c05815>, 2021.

697 Huang, Z. J., Zheng, J. Y., Qu, J. M., Zhong, Z. M., Wu, Y. Q., Shao, M.: A Feasible Methodological  
698 Framework for Uncertainty Analysis and Diagnosis of Atmospheric Chemical Transport  
699 Models, *Environ. Sci. Technol.*, 53, 3110-3118, <https://doi.org/10.1021/acs.est.8b06326>, 2019.

700 Ji, Z., Gan, M., Fan, X., Chen, X., Li, Q., Lv, W., Tian, Y., Zhou, Y., Jiang, T.: Characteristics of  
701 PM<sub>2.5</sub> from iron ore sintering process: Influences of raw materials and controlling methods, *J.*  
702 *Clean. Prod.*, 148, 12-22, <https://doi.org/10.1016/j.jclepro.2017.01.103>, 2017.

703 Li, J., Wu, Y., Ren, L., Wang, W., Tao, J., Gao, Y., Li, G., Yang, X., Han, Z., Zhang, R.: Variation in  
704 PM<sub>2.5</sub> sources in central North China Plain during 2017–2019: Response to mitigation  
705 strategies, *J. Environ. Manage.*, 28, 112370, <https://doi.org/10.1016/j.jenvman.2021.112370>,  
706 2021.

707 Li, M., Hu, M., Du, B., Guo, Q., Tan, T., Zheng, J., Huang, X., He, L., Wu, Z., Guo, S.: Temporal  
708 and spatial distribution of PM<sub>2.5</sub> chemical composition in a coastal city of Southeast China, *Sci.*  
709 *Total Environ.*, 605-606, 337-346, <https://doi.org/10.1016/j.scitotenv.2017.03.260>, 2017a.

710 Li, M., Liu, H., Geng, G., Hong, C., Liu, F., Song, Y., Tong, D., Zheng, B., Cui, H., Man, H., Zhang,  
711 Q., He, K.: Anthropogenic emission inventories in China: a review, *Natl. Sci. Rev.*, 4, 834-866,  
712 <https://doi.org/10.1093/nsr/nwy044>, 2017b.

713 Li, X., He, K., Li, C., Yang, F., Zhao, Q., Ma, Y., Chen, Y., Ouyang, W., Chen, G.: PM<sub>2.5</sub> mass,  
714 chemical composition, and light extinction before and during the 2008 Beijing Olympics, *J.*  
715 *Geophys. Res.*, 118, 12158-12167, <https://doi.org/10.1002/2013JD020106>, 2013.

716 Liang, F., Xiao, Q., Yang, X., Liu, F., Li, J., Lu, X., Liu, Y., Gu, D.: The 17-y spatiotemporal trend  
717 of PM<sub>2.5</sub> and its mortality burden in China, *Proc. Natl. Acad. Sci.*, 117, 25601-25608,  
718 <https://doi.org/10.1073/pnas.1919641117>, 2020.

719 Lv, L., Wei, P., Li, J., Hu, J.: Application of machine learning algorithms to improve numerical  
720 simulation prediction of PM<sub>2.5</sub> and chemical components, *Atmos. Pollut. Res.*, 12, 101211,  
721 10.1016/j.apr.2021.101211, 2021.

722 NBS (National Bureau of Statistics of China): China Statistical Yearbook 2021,  
723 <http://www.stats.gov.cn/tjsj/ndsj/2021/indexch.htm>, last access: 2022.

724 Peterson, G., Hogrefe, C., Corrigan, A., Neas, L., Mathur, R., Rappold, A.: Impact of Reductions in  
725 Emissions from Major Source Sectors on Fine Particulate Matter–Related Cardiovascular  
726 Mortality, *Environ. Health Persp.*, 128, 017005, <https://doi.org/10.1289/EHP5692>, 2020.

727 Qi, H., Cui, C., Zhao, T., Bai, Y., Liu, L.: Numerical simulation on the characteristics of PM<sub>2.5</sub> heavy  
728 pollution and the influence of weather system in Hubei Province in winter 2015 (In Chinese),  
729 *Meteorological monthly*, 45, 1113-1122, <https://doi.org/10.7519/j.issn.1000-0526.2019.08.008>,  
730 2019.

731 Seinfeld, J. H., Pandis, S. N.: Atmospheric Chemistry and Physics, from air pollution to climate  
732 change. John Wiley & Sons, Inc., Hoboken, New Jersey.47-61, ISBN9781119221166, 2006

733 Sha, T., Ma, X., Jia, H., Tian, R., Chang, Y., Cao, F., Zhang, Y.: Aerosol chemical component:  
734 Simulations with WRF-Chem and comparison with observations in Nanjing, Atmos. Environ.,  
735 218, 1-14, <https://doi.org/10.1016/j.atmosenv.2019.116982>, 2019.

736 Shi, W., Liu, C., Norback, D., Deng, Q., Huang, C., Qian, H., Zhang, X., Sundell, J., Zhang, Y., Li,  
737 B., Kan, H., Zhao, Z.: Effects of fine particulate matter and its constituents on childhood  
738 pneumonia: a cross-sectional study in six Chinese cities, Lancet, 392, S79,  
739 [https://doi.org/10.1016/S0140-6736\(18\)32708-9](https://doi.org/10.1016/S0140-6736(18)32708-9), 2018.

740 Shi, Z., Li, J., Huang, L., Wang, P., Wu, L., Ying, Q., Zhang, H., Lu, L., Liu, X., Liao, H., Hu, J.:  
741 Source apportionment of fine particulate matter in China in 2013 using a source-oriented  
742 chemical transport model, Sci. Total Environ., 601-602, 1476-1487,  
743 <https://doi.org/10.1016/j.scitotenv.2017.06.019>, 2017.

744 Song, S. Y., Wang, Y. S., Wang, Y. L., Wang, T., Tan, H. Z.: The characteristics of particulate matter  
745 and optical properties of Brown carbon in air lean condition related to residential coal  
746 combustion, Powder Technol., 379, 505-514, <https://doi.org/10.1016/j.powtec.2020.10.082>,  
747 2021.

748 Tang, X. Y., Zhang, Y. H., Shao, M.: Atmosphere Environment Chemistry, Second ed (In Chinese). .  
749 Higher Education Press, Beijing, China.268-329, ISBN978-7-04-019361-9, 2006

750 Wang, C., Zheng, J., Du, J., Wang, G., Klemes, J., Wang, B., Liao, Q., Liang, Y.: Weather condition-  
751 based hybrid models for multiple air pollutants forecasting and minimisation, J. Clean. Prod.,  
752 352, 131610, <https://doi.org/10.1016/j.jclepro.2022.131610>, 2022.

753 Wang, D., Hu, J., Xu, Y., Lv, D., Xie, X., Kleeman, M., Xing, J., Zhang, H., Ying, Q.: Source  
754 contributions to primary and secondary inorganic particulate matter during a severe wintertime  
755 PM<sub>2.5</sub> pollution episode in Xi'an, China, Atmos. Environ., 97, 182-194,  
756 <https://doi.org/10.1016/j.atmosenv.2014.08.020>, 2014.

757 Weagle, C., Sinder, G., Li, C. C., Donkelaar, A., S, P., Bissonnette, P., Burke, I., Jackson, J., Latimer,  
758 R., Stone, E., Abboud, I., Akoshile, C., Anh, N., Brook, J., Cohen, A., Dong, J., Gibson, M.,  
759 Griffith, D., He, K., Holben, B., Kahn, R., Keller, C., Kim, J., Lagrosas, N., Lestari, P., Khian,  
760 Y., Liu, Y., Marais, E., Martins, J., Misra, A., Muliane, U., Pratiwi, R., Quel, E., Salam, A.,  
761 Segey, L., Tripathi, S., Wang, C., Zhang, Q., Brauer, M., Rudich, Y., Martin, R.: Global Sources  
762 of Fine Particulate Matter: Interpretation of PM<sub>2.5</sub> Chemical Composition Observed by  
763 SPARTAN using a Global Chemical Transport Model, Environ. Sci. Technol., 52, 11670-11681,  
764 <https://doi.org/10.1021/acs.est.8b01658>, 2018.

765 Wongphatarakul, V., Friedlander, S. K., Pinto, J. P.: A Comparative Study of PM<sub>2.5</sub> Ambient Aerosol  
766 Chemical Databases, Environ. Sci. Technol., 32, 3926-3934,  
767 <https://doi.org/10.1021/es9800582>, 1998.

768 Wu, B., Bai, X., Liu, W., Zhu, C., Hao, Y., Lin, S., Liu, S., Luo, L., Liu, X., Zhao, S., Hao, J., Tian,  
769 H.: Variation characteristics of final size-segregated PM emissions from ultralow emission  
770 coal-fired power plants in China, Environ. Pollut., 259, 113886,  
771 <https://doi.org/10.1016/j.envpol.2019.113886>, 2020.

772 Wu, D., Zheng, H., Li, Q., Jin, L., Lyu, R., Ding, X., Huo, Y., Zhao, B., Jiang, J., Chen, J., Li, X.,  
773 Wang, S.: Toxic potency-adjusted control of air pollution for solid fuel combustion, Nat. Energy,  
774 7, 194-202, <https://doi.org/10.1038/s41560-021-00951-1>, 2022.

775 Wu, Z. X., Hu, T. F., Hu, W., Shao, L. Y., Sun, Y. Z., Xue, F. L., Niu, H. Y.: Evolution in  
776 physicochemical properties of fine particles emitted from residential coal combustion based on  
777 chamber experiment, *Gondwana Res.*, <https://doi.org/10.1016/j.gr.2021.10.017>, 2021.

778 Xia, Z. Q., Fan, X. L., Huang, Z. J., Liu, Y. C., Yin, X. H., Ye, X., Zheng, J. Y.: Comparison of  
779 Domestic and Foreign PM<sub>2.5</sub> Source Profiles and Influence on Air Quality Simulation (In  
780 Chinese), *Res. Environ. Sci.*, 30, 359-367, <https://doi.org/10.13198/j.issn.1001-6929.2017.01.55>, 2017.

781

782 Yang, F., Tan, J., Zhao, Q., Du, Z., He, K., Ma, Y., Duan, F., Chen, G., Zhao, Q.: Characteristics of  
783 PM<sub>2.5</sub> speciation in representative megacities and across China, *Atmos. Chem. Phys.*, 11, 1025-  
784 1051, <https://doi.org/10.5194/acpd-11-1025-2011>, 2011.

785 Ying, Q., Feng, M., Song, D. L., Wu, L., Hu, J., Zhang, H., Kleeman, M., Li, X.: Improve regional  
786 distribution and source apportionment of PM<sub>2.5</sub> trace elements in China using inventory-  
787 observation constrained emission factors, *Sci. Total Environ.*, 624, 355-365,  
788 <https://doi.org/10.1016/j.scitotenv.2017.12.138>, 2018.

789 Yu, S. C., Mathur, R., Pleim, J., Wong, D., Gilliam, R., Alapaty, K., Zhao, C., Liu, X.: Aerosol  
790 indirect effect on the grid-scale clouds in the two-way coupled WRF-CMAQ: model  
791 description, development, evaluation and regional analysis, *Atmos. Chem. Phys.*, 14, 11247-  
792 11285, <http://10.5194/acp-14-11247-2014>, 2014.

793 Yu, Z. C., Jang, M., Kim, S., Bae, C., Koo, B., Beardsley, R., Park, J., Chang, L., Lee, H., Lim, Y.,  
794 Cho, J.: Simulating the Impact of Long-Range-Transported Asian Mineral Dust on the  
795 Formation of Sulfate and Nitrate during the KORUS-AQ Campaign, *Earth Space Chem.*, 4,  
796 1039-1049, <https://doi.org/10.1021/acsearthspacechem.0c00074>, 2020.

797 Zhang, J., Wu, J., Lv, R., Song, D., Huang, F., Zhang, Y., Feng, Y.: Influence of Typical  
798 Desulfurization Process on Flue Gas Particulate Matter of Coal-fired Boilers (In Chinese),  
799 *Environ. Sci.*, 41, 4455-4461, <https://doi.org/10.13227/j.hjcx.202003193>, 2020.

800 Zhang, Q., Xue, D., Wang, S., Wang, L., Wang, J., Ma, Y., Liu, X.: Analysis on the evolution of  
801 PM<sub>2.5</sub> heavy air pollution process in Qingdao (In Chinese), *China Environ. Sci.*, 37, 3623-3635,  
802 <https://doi.org/10.3969/j.issn.1000-6923.2017.10.003>, 2017.

803 Zhang, S. P., Xing, J., Sarwar, G., Ge, Y. L., He, H., Duan, F., Zhao, Y., He, K., Zhu, L., Chu, B.:  
804 Parameterization of heterogeneous reaction of SO<sub>2</sub> to sulfate on dust with coexistence of NH<sub>3</sub>  
805 and NO<sub>2</sub> under different humidity conditions, *Atmos. Environ.*, 208, 133-140,  
806 <https://doi.org/10.1016/j.atmosenv.2019.04.004>, 2019.

807 Zheng, B., Tong, D., Li, M., Liu, F., Hong, C., Geng, G., Li, H., Li, X., Peng, L., Qi, J., Yan, L.,  
808 Zhang, Y., Zhao, H., Zheng, Y., He, K., Zhang, Q.: Trends in China's anthropogenic emissions  
809 since 2010 as the consequence of clean air actions, *Atmos. Chem. Phys.*, 18, 14095-14111,  
810 <https://doi.org/10.5194/acp-18-14095-2018>, 2018.

811 Zheng, B., Zhang, Q., Zhang, Y., He, K. B., Wang, K., Zheng, G. J., Duan, F. K., Ma, Y. L., Kimoto,  
812 T.: Heterogeneous chemistry: a mechanism missing in current models to explain secondary  
813 inorganic aerosol formation during the January 2013 haze episode in North China, *Atmos.*  
814 *Chem. Phys.*, 15, 2031-2049, [10.5194/acp-15-2031-2015](https://doi.org/10.5194/acp-15-2031-2015), 2015.

815 Zheng, H., Song, S., Sarwar, G., Gen, M., Wang, S., Ding, D., Chang, X., Zhang, S., Xing, J., Sun,  
816 Y. L., Ji, D., Chan, C. K., Gao, J., McElroy, M.: Contribution of Particulate Nitrate Photolysis  
817 to Heterogeneous Sulfate Formation for Winter Haze in China, *Environ. Sci. Technol. Lett.*, 7,  
818 632-638, <https://doi.org/10.1021/acs.estlett.0c00368>, 2020.

819 Zhou, L., Chen, X., Tian, X.: The impact of fine particulate matter (PM<sub>2.5</sub>) on China's agricultural  
820 production from 2001 to 2010, J. Clean. Prod., 178, 133-141,  
821 <https://doi.org/10.1016/j.jclepro.2017.12.204>, 2018.  
822